



Main Manuscript for

ACBP/DBI protein neutralization confers autophagy-dependent organ protection through inhibition of cell loss, inflammation and fibrosis

Omar Motiño¹⁻², Flavia Lambertucci^{1-2*}, Gerasimos Anagnostopoulos^{1-3*}, Sijing Li^{1-3*}, Jihoon Nah⁴, Francesca Castoldi⁵, Laura Senovilla^{1-2,6}, Léa Montégut¹⁻³, Hui Chen¹⁻², Sylvère Durand¹⁻², Mélanie Bourgin¹⁻², Fanny Aprahamian¹⁻², Nitharsshini Nirmalathasan¹⁻², Karla Alvarez-Valadez¹⁻³, Allan Sauvat¹⁻², Vincent Carbonnier¹, Mojgan Djavaheri-Mergny¹⁻², Federico Pietrocola⁵, Junichi Sadoshima⁴, Maria Chiara Maiuri¹⁻², Isabelle Martins^{1-2#}, and Guido Kroemer^{1-2, 7-8#}

¹ Centre de Recherche des Cordeliers, Equipe labellisée par la Ligue contre le cancer, Université de Paris, Sorbonne Université, Inserm U1138, Institut Universitaire de France, Paris, France.

² Metabolomics and Cell Biology Platforms, Institut Gustave Roussy, Villejuif, France.

³ Faculté de Médecine, Université de Paris Saclay, Kremlin Bicêtre, France.

⁴ Department of Cell Biology & Molecular Medicine, New Jersey Medical School- Rutgers, The State University of New Jersey, Newark, NJ, USA.

⁵ Department of Bioscience and Nutrition, Karolinska Institute, Huddinge, Sweden.

⁶ Unidad de Excelencia Instituto de Biología y Genética Molecular (IBGM), Universidad de Valladolid - CSIC, Valladolid, Spain.

⁷ Pôle de Biologie, Hôpital Européen Georges Pompidou, AP-HP, Paris, France.

⁸ Lead contact.

#Correspondence: Guido Kroemer (Kroemer@orange.fr) or Isabelle Martins (isabelle.martins@inserm.fr).

*These authors contributed equally to this work.

Supplemental information

Material and Methods

Chemicals and reagents

Reagents were obtained from Axon Medchem BV (Groningen, Netherlands), Qiagen (Hilden, Germany), Millipore (MA, USA), Randox (Antrim, UK), Roche Applied Science (Upper Bavaria, Germany) and Sigma Aldrich (MO, USA). Reagents for electrophoresis were obtained from Thermo Fisher Scientific (MA, USA) and BioRad (CA, USA). Antibodies were from Abcam (TX, USA), Abnova (Taipei, Taiwan), Cell Signaling (MA, USA) and Sigma Aldrich.

Biochemical assays

Plasma ALT and AST activity was determined by colorimetric kits (Randox) accordingly with the manufacturer's instructions. The levels of cytokine were measured by Luminex analysis (Luminex FlexMap 3D). To quantify collagen, hepatic hydroxyproline content was assayed by means of a commercial kit (Sigma Aldrich).

Animal experimentation

Wild-type (*Wt*) C57BL/6 mice (Envigo, Gannat, France), homozygous *Atg4b*^{-/-} mice (gift of Dr. Carlos Lopez-Otin, University of Oviedo, Spain), tamoxifen-inducible whole-body knockout of floxed *Acbp/Dbi*^{-/-} mice (*UBC-cre/ERT2::Acbp/Dbi*^{fl/fl}, control: *Acbp/Dbi*^{fl/fl} without CRE) (1), homozygous *Gabrg2*^{mut/mut} mice (bearing a point mutation F77I in the binding site of ACBP/DBI in the gamma-aminobutyric acid A Receptor $\gamma 2$ subunit) (2), and transgenic mice expressing LC3 conjugated to green fluorescent protein (GFP-LC3-Tg) (3) were bred and maintained according to the FELASA guidelines and local guidelines from the Animal Experimental Ethics Committee (Permissions #25000, #31411, #34537, #34538, and #34539). Homozygous *Atg7*^{-/-} (*Atg7*^{fl/fl}, α MHC *Cre*⁺, control: *Atg7*^{fl/fl}, α MHC *Cre*⁻) and Mito-Keima transgenic mice (4) were used according to the National Institutes of Health guide for the care and use of laboratory animals (NIH Publications No. 8023, revised 1978). Mice were housed in a temperature-controlled environment with 12 h light/dark cycles and were fed with diet and water ad libitum. All animals were sacrificed, and the heart, liver and lung were snap-frozen in liquid nitrogen and stored at -80°C, or fixed in 4% buffered paraformaldehyde overnight at 4°C and embedded in paraffin. Plasma was obtained by cardiac puncture.

Neutralization of DBI by passive or active immunization

The monoclonal antibody against DBI (passive immunization) or isotype IgG (Bioxcell, NH, USA) was used in vivo (2.5 μ g/g body weight, B.W., intraperitoneally, i.p., in 200 μ L) in a single or several

doses. In some experiment, leupeptin (Leu, 30 mg/kg B.W.) was injected i.p. injection 2 h before the end of the experiment.

The production of autoantibodies (active immunization) was induced by conjugation of Keyhole limpet hemocyanin (KLH; from Thermo) and mouse recACBP (KLH-DBI) as Montégut *et al.* described (5). Briefly, KLH and DBI were mixed at a 1:20 molar ratio and adjusted gradually to 0.25% (v/v) glutaraldehyde. After, the glycine solution was added to finish the reaction, and was ultra-filtrated using a 100 KDa membrane (Millipore). A solution of formaldehyde was added to 0.2% (v/v) final concentration, and the reaction was quenched by addition of a glycine solution followed by an ultrafiltration with 70 mM pH 7.8 phosphate buffer. Male 8-week-old C57BL/6 mice were immunized with i.p. injection of 30, 30, 30, 10 μ g of KLH-DBI or KLH alone as an adjuvant emulsion (1:1) with Montanide ISA-51vg (Seppic, Paris, France) on days 0, 7, 14 and 21, respectively.

Cardiac injury *in vivo*

Male three-month-old *Wt* and *Atg7^{-/-}* mice were anesthetized by i.p. injection of 60 μ g/g pentobarbital sodium and subjected to 3 hours of ischemia by permanent left anterior descending coronary artery (LAD) ligation (6) After sacrifice, hearts were harvested and subjected to 1% Alcian Blue and 1% TTC (2,3,5-triphenyltetrazolium chloride) staining by perfusion (7).

Acute liver damage in mice

To induce hepatic ischemia reperfusion injury, male 12-week-old C57BL/6 mice were anesthetized with 2% isoflurane, and a model of segmental (70%) warm hepatic I/R protocol was assessed (8). Briefly, liver ischemia was induced for 90 min, and reperfusion was initiated by removal of the clamp for 4 hours. To induce hepatotoxicity, male 12-week-old C57BL/6 mice were treated with 12 mg/kg Concanavalin A (ConA, Sigma Aldrich) or 300 mg/kg acetaminophen (APAP, Sigma Aldrich) for 4 or 16 hours, respectively. For inhibition of the autophagy flux, the animals were injected i.p. with two doses of 50 mg/kg hydroxychloroquine (HCQ, in PBS; Axon Medchem BV) 4 hours and just before the hepatic damage.

NASH and hepatic fibrosis model *in vivo*

Male 2-3 months old mice were fed with regular chow diet (RCD) or methionine choline-deficient diet (MCD; AIN-76 Safe diet, Essingen, Germany) for 4 weeks as preventive model (prophylaxis). Some mice were fed with MCD diet for 4 weeks and then with RCD diet for another 4 days as a diet recovery model (reversion, R). For inhibition of β -oxidation, etomoxir (ETO, Sigma Aldrich) was injected i.p. 2 hours after R and then daily into C57BL/6 mice. To induce fibrosis in the liver, CCl₄ (Sigma Aldrich) was i.p. administered to male 2-months-old C57BL/6 mice at a dose of 1.6 ml/kg

twice weekly for 9 weeks (9). Control animals were i.p. injected with the vehicle olive oil (Sigma Aldrich). Additional groups were administrated i.p. with 50 mg/kg HCQ daily for the four last weeks of CCl₄. Another approach to induce hepatic fibrosis involved by bile duct ligation (BDL) for 2 weeks (10).

Pulmonary fibrosis in mice

To induce lung fibrosis, male 2-3 months old was administrated intratracheally with one single dose of 2 mg/kg bleomycin and the animals were sacrificed after 18 days (11).

Histopathology

Paraffin-embedded sections (5 µm) were stained with hematoxylin-eosin-safranin (HES) or Sirius Red and were evaluated by experienced pathologist blinded to the features of the animal groups. All slides were scanned with an AxioScan Z1 (Carl Zeiss, Jena, Germany). The NAFLD activity score was assessed using the NAFLD scoring system for mice models validated by Liang *et al.* (12). Briefly, steatosis grade was grouped as follows: grade 0, <5% of steatotic hepatocytes; grade 1, 5–33%; grade 2, 33–66%; and grade 3, >66%. Lobular inflammation was scored as follows: 0, no foci; 1, <2 foci; 2, 2–4 foci; and 3, >4 foci. Ballooning was classified as 0, none; 1, few balloon cells; and 2, many balloon cells. NAFLD activity score was calculated for each liver biopsy based on the sum of scores for steatosis, inflammation, and ballooning. In addition, liver fibrosis staging (Metavir score) was defined as 0, none; 1, perisinusoidal and/or pericentral; 2, incomplete central/central bridging fibrosis; 3, complete central/central bridging fibrosis; and 4, definite cirrhosis (13). The severity of hepatic IR was graded according to Suzuki's criteria on a scale from 0 to 4. None (0%), minimal (10%), mild (11-30%), moderate (30-60 %) and severe (>60%) necrosis, congestion, or centro-lobular ballooning was assigned as grade 0, 1, 2, 3 and 4, respectively (14). To measure APAP hepatotoxicity, liver samples were classified as none (0; 0%), mild (1; less than 20%), moderate (2; 20 ~ 70%), severe (3; more than 70% of hepatic lobules), taking account of the cell death area, ballooning, and inflammation around the central veins (15). The hepatic injury induced by ConA was scored using grades as follows: 0, no necrotic infiltrates; 1, small foci of necrotic cells between hepatocytes or necrotic cells surrounding individual hepatocytes; 2, larger foci of 100 necrotic cells or involving 30 hepatocytes; 3, 10% of a hepatic cross-section involved; and 4, 30% of a hepatic cross-section involved (Zhao *et al.*, 2020). The pulmonary damage/fibrosis was assessed by the Ashcroft score: 0, normal lung; 1, minimal fibrosis thickening of wall without obvious damage to lung architecture; 3, moderate fibrosis thickening of wall without obvious damage to lung architecture; 5, increased fibrosis with definite damage to lung structure and formation of fibrous bands or fibrous small masses; 7, severe distortion of structure and large fibrosis areas ("Honeycomb lung" is placed in this category); and 8, total fibrous obliteration of the

field (17). Also, to determinate the abundance of hepatic macrophages and Kupffer cells, liver sections from fixed paraffin blocks were immunohistochemically stained according to standard procedures using anti-mouse F4/80.

Liver extracts

For protein or RNA extraction, tissues were homogenized in 2 cycles for 20 s at 5,500 rpm using a Precellys 24 tissue homogenator (Bertin Technologies, Montigny-le-Bretonneux, France) in 20 mM Tris buffer (pH 7.4) containing 150 mM NaCl, 1% Triton X-100, 10 mM EDTA and Complete® protease inhibitor cocktail (Roche Applied Science) or QIAzol (Qiagen), respectively. After, protein extracts were centrifuged at 12,000 g (4 °C) for 15 min and supernatants were collected. Protein concentration in supernatants was evaluated by the bicinchoninic acid technique (BCA protein assay kit, Thermo Fisher Scientific). Homogenate RNA was purified with RNeasy Mini Kit (Qiagen) following the manufacturer's instructions. The purify and concentration of RNA was measured by NanoDrop™ (Thermo Fisher Scientific).

Whole transcriptome analysis

For RNA-sequencing library preparation, RNA was extracted from mouse livers using RNA Plus Mini Kit (Qiagen) according to manufacturer's instructions. The concentration and integrity of total RNA was analyzed using electrophoretic separation on microfabricated chips in Agilent 2100 Bioanalyzer System (Agilent, CA, USA). After, mRNA-sequencing library preparation (1.5 µg total RNA per sample) was carried out on NovaSeq 6000 PE150 instrument (2 x 150 bp, 40 million reads per sample). For RNA-sequencing data analysis, pseudo-alignment and quantification were carried-out with HISAT2 algorithm (reference genome GRCm39) (18). Then, the correlation analysis of the principal component study and differential expression analysis were performed with DESeq2 package (19). To study the differential gene expression, the analyses were ran using the parametric Wald test with Benjamini-Hochberg adjustment (p -adj). Genes were expressed using Z-Score normalization and were considered significantly differentially expressed when p -adj < 0.05 and \log^2 (fold change) (cut-off) was $\geq \pm 1.5$. GSEA (Gene Set Enrichment Analysis), based gene ontology (GO) and Kyoto Encyclopedia of Genes and Genomes (KEGG) analyses were performed on RNA-seq data from liver samples (20). A web-based bioinformatics tool (<http://www.bioinformatics.com.cn>) was used to draw the graph.

Analysis of GEO datasets

The genes over-expressed in human liver samples from NAFLD/NASH compared with normal livers in ten Gene Expression Omnibus (GEO) datasets (GSE159676, GSE151158, GSE63067, GSE48452, GSE17470, GSE66676, GSE24807, GSE33814, GSE126848, and GSE135251) were

identified by the GEO2R tool or the stats package in R software (version 4.1.0). The genes reduced by α -DBI in MCD experiments were detected by the stats package in R software. The overlap of genes between datasets, α -DBI down-regulates genes that are upregulated in human NAFLD/NASH, were selected by means of a Venn diagram. The overlap representation factor (ORF) is the ratio between actual overlap on theoretical overlap, which is calculated by the formula $ORF = x * N / (n1 * n2)$, with x =number of genes in common between two groups, N =total unique genes of two groups, $n1$ =number of genes in group 1, $n2$ =number of genes in group 2. The p value was calculated by means Fisher's exact test.

Gene expression analyses

Total RNA (1 μ g) was reverse transcribed using the SuperScript™ VILO™ cDNA Synthesis Kit (Invitrogen). Quantitative real-time PCR was performed with a StepOnePlus Real-Time PCR System (Applied Biosystems, Thermo Fisher Scientific) sequence detector using the Master Mix PCR Power SYBR™ Green (Applied Biosystems, Thermo Fisher Scientific) and d(N)6 random hexamer with the primers described in the Table S2. Specific primers were purchased from Sigma. PCR thermocycling parameters were 95 °C for 1min, 40 cycles of 95 °C for 15 s, and 60 °C for 1 min. Each sample was run in duplicate and was normalized to 36b4 mRNA expression levels. Then, the replicates were averaged, and fold induction was determined as $\Delta\Delta$ Ct based fold-change.

Western Blots

For immunoblotting, whole-cell extracts were boiled for 5 min in Laemmli sample buffer, and equal amounts of protein (20–30 μ g) were separated on 4-12% Bis-Tris acrylamide precast gels (Thermo Fisher Scientific) and electro-transferred to PDVF membranes (BioRad). Membranes were horizontally sliced according to the molecular weight of the protein of interest to allow simultaneous detection within the same experiment. Unspecific binding sites were saturated by incubating membranes for 1 h in 0.05% Tween 20 (v:v in TBS) supplemented with 5% non-fat powdered milk (w:v in TBS). The relative amount of each protein was determined by overnight incubation with primary antibodies specific for ACBP/DBI, α -SMA, ATG4B, CATALASE, CPT1A, COLLAGEN 1A1, HMOX1, MAP1LC3B/LC3B, PPAR- α , SOD2, and SQSTM1/p62 (Table S2). Glyceraldehyde-3-phosphate dehydrogenase antibody (Table S2) was used to control equal loading of lanes. The blots were revealed with appropriate horseradish peroxidase (HRP)-labeled secondary antibodies (Southern Biotech, AL, USA) plus SuperSignal West Pico chemoluminescent substrate (Thermo Fisher Scientific) and different exposition times were performed for each blot with a charged coupling device camera in a luminescent image analyzer LAS 4000 (GE Healthcare, IL, USA) to ensure the linearity of the band intensities. Densitometric analysis of the bands was carried out using ImageJ software (<http://imagej.nih.gov>) and expressed in relative expression.

Quantitative analysis of autophagy biosensors in tissues

Hearts from Mito-Kemia transgenic mice and liver from LC3-GFP transgenic mice were collected and fixed with 4% paraformaldehyde (in PBS, pH 7.4) for at least 16 h, followed by treatment with 30% sucrose (in PBS) overnight at 4°C. Samples were embedded in Tissue-Tek OCT compound (Sakura Finetechnical, Tokyo, Japan) and stored at -80 °C. Five µm-thick tissue sections were prepared with a Cryostat CM3050S S cryostat (Leica Microsystems), air-dried for at least 1 hour, washed in PBS for 5 min, dried at RT for 30 min, and mounted with DAPI Fluoromount-G® anti-fading medium (SouthernBiotech, AL, USA). Then, the slides were scanned using a LSM 710 confocal fluorescence microscope (Carl Zeiss, Jena, Germany). Livers or hearts from mice expressing GFP-LC3 were subjected to a similar histological analysis. GFP-LC3 dots were quantified in three independent visual fields from at least three mice per group, using Image J software.

Metabolomics liver sample preparation

First, 30 mg of livers were weighted and transferred to 2 mL-homogenizer tube with ceramic beads (Hard Tissue Homogenizing CK28, 2.8 mm zirconium oxide beads; Precellys, Bertin Technologies), containing 1 mL of ice-cold extraction mixture (metOH/water, 9/1, -20°C, with a cocktail of internal standards). To facilitate solvent access and endogenous metabolites extraction, samples were completely homogenized in Precellys 24 tissue homogenize (3 cycles of 20 s/ 5000 rpm). After centrifugation (10 min at 15000 g, 4°C), supernatants were collected. For plasma, samples (25 µL) were mixed with 250 µL of the of ice-cold extraction mixture, allowing protein precipitation and metabolites extraction, then vortexed and centrifuged (10 min at 15000 g, 4°C). Next, tissues or plasma centrifugation, supernatants were collected, split in 3 fractions, and treated following published protocols (21). Briefly, they extract were split in 3 fractions: first fraction for short chain fatty acids analysis (40 µL for both tissues and plasma samples) were derivatized before injection, 2nd fraction for LC/MS and 3d fraction for GC/MS analyses (300 µL/each for tissue and 100 µL/each for plasma samples) were transferred to an injection amber glass vial (with fused-in insert) and evaporated to dryness (Techne DB3, Staffordshire, UK) at 40°C. The second dried fraction was recovered with 200 µL or 150 µL (tissue or plasma samples, respectively) of ultra-pure water and kept at -80°C until injection and analysis by LC/MS. The third dried fraction was derivatized before GC/MS injection and analysis. Finally, the 4th fraction together with the sample pellet were re-extracted with an equal volume of 2% SSA (in methanol), vortexed and centrifuged (10 min at 15000 g, 4°C). The supernatant (350 and 60 µL, from tissue and plasma extracts, respectively) was transferred to an injection polypropylene vial (with fused-in insert) and evaporated to dryness (Techne DB3, Staffordshire, UK) at 40°C. Dried samples were dissolved with ultra-pure water (200

and 100 μ L, for tissue and plasma dried extracts, respectively) and kept at -80°C until injection and analysis by UHPLC/MS for polyamines detection.

Metabolomic analysis

Targeted analysis of nucleoside phosphates and cofactors by ion pairing Ultra-High Performance Liquid Chromatography (UHPLC) coupled to a Triple Quadrupole (QQQ) mass spectrometer: Targeted UHPLC/MS analyses were performed on a UHPLC 1290 system (Agilent), with an autosampler kept at 4°C , and a pellet oven for rigorous control of the column temperature. The UHPLC was coupled to a QQQ/MS 6470 (Agilent) equipped with an electrospray source, using nitrogen as collision gas. Short chain fatty acids and ketones bodies were detected in the 1st fraction after injection of 10 μ L of sample were into a Zorbax Eclipse XDB-C18 (100 mm x 2.1 mm, particle size 1.8 μm ; Agilent) column protected by a guard column C18 (5 mm x 2.1 mm, particle size 1.8 μm). Column oven maintained at 50°C during analysis. The gradient mobile phase consisted of 0.01 % formic acid (Sigma Aldrich) (A) and ACN (0.01 % formic acid) (B). The flow rate was set to 0.7 ml/min, and gradient as follow: 20% B (initial conditions) maintained for 3 min, to 45% B in 4 min; then 95% B maintained 2 min, and finally equilibration to initial conditions, 20% B, for 1 min. The QQQ/MS was operated in negative mode. The gas temperature was set to 300°C with a gas flow of 12 L/min. The capillary voltage was set to 5 kV.

For bile acid detection, 5 μ L from samples recovered in water (2nd fraction), were injected into a Poroshell 120 EC-C8 (100 mm x 2.1 mm particle size 2.7 μm ; Agilent technologies) column protected by a guard column (XDB-C18, 5 mm x 2.1 mm particle size 1.8 μm). Mobile phase consisted of 0.2% formic acid (A) and ACN/IPA (1/1; v/v) (B) freshly made. Flow rate was set to 0.5 mL/min, and gradient as follow: 30% B increased to 38% B over 2 min; maintained for 2 min then increased 60% for 1.5 minutes, and finally to 98% B for 2 minutes (column washing), followed by 2 min of column equilibration at 30% B (initial conditions). The QQQ/MS was operated in negative mode. Gas temperature and flow were set to 310°C and 12 L/min, respectively. Capillary voltage was set to 5 kV. Polyamines were detected in the 4th fraction after injection of 10 μ L of sample were into a Kinetex C18 (150 mm x 2.1 mm particle size 2.6 μm ; Phenomenex) column protected by a guard column C18 (5 mm x 2.1 mm, particle size 1.8 μm). Column oven maintained at 40°C during analysis. The gradient mobile phase consisted of 0.1 % HFBA (Sigma) (A) and ACN (0.1 % HFBA) (B) freshly made. The flow rate was set to 0.4 ml/min, and gradient as follow: from 5% (initial conditions) to 30% B in 7 min; then 90% B maintained 2 min, and finally equilibration to initial conditions, 5% B, for 2 min. The QQQ/MS was operated in positive mode. The gas temperature was set to 350°C with a gas flow of 12 L/min. The capillary voltage was set to 2.5 kV. In addition, tissue samples were injected for the analysis of nucleotides and co-factors into a Zorbax Eclipse plus C18 (100 mm x 2.1 mm, particle size 1.8 μm , Agilent) column protected by a guard column

C18 (5 mm × 2.1 mm, particle size 1.8 µm). Column oven maintained at 40°C during analysis. The gradient mobile phase consisted of 0.5 mM DBAA (Sigma) (A) and ACN (B). The flow rate was set to 0.4 mL/min, and gradient as follow: 10% B (initial conditions) maintained for 3 min, then increased to 95% B in 1 min and maintained 2 min, to finally equilibrate to initial conditions, 10% B, for 1 min. The QQQ/MS was operated in both positive and negative mode. The gas temperature was set to 350°C with a gas flow of 12 L/min. The capillary voltage was set to 4.5 kV in positive mode and 5 kV in negative mode. MRM scan mode was used for targeted analysis in both GC and UHPLC/MS. Peak detection and integration were performed using the Agilent Mass Hunter quantitative software (B.10.1).

Widely targeted analysis of intracellular metabolites. GC/MS: Derivatized samples for GC/MS analysis (3d fraction) were injected (1 µL) into a gas chromatograph (Agilent 7890B; Agilent Technologies, Waldbronn, Germany) coupled to a triple quadrupole mass spectrometer (QQQ/MS; 7000C Agilent Technologies, Waldbronn, Germany), equipped with a high sensitivity electronic impact source (EI) operating in positive mode. Injection was performed in splitless mode. Front inlet temperature was kept at 250°C, transfer line and ion-source temperature were 250°C and 230°C, respectively. Septum purge flow was fixed at 3 mL/min, purge flow to split vent operated at 80 mL/min during 1 min and gas saver mode was set to 15 mL/min after 5 min. Helium gas flowed through column (HP-5MS, 30m x 0.25 mm, i.d. 0.25 mm, d.f. J&WScientific, Agilent Technologies Inc.) at 1 mL/min. Column temperature was held at 60°C for 1 min, raised to 210°C (10°C/min), then to 230°C (5°C/min), to finally reach 325°C (15°C/min). The collision gas was nitrogen.

Pseudo-targeted analysis of intracellular metabolites. UHPLC/MS: The profiling analysis was performed with a Dionex Ultimate 3000 UHPLC system (Thermo Fisher Scientific) coupled to an Orbitrap mass spectrometer (q-Exactive, Thermo Fisher Scientific) equipped with an electrospray source operating in both positive and negative mode, and acquired samples in full scan analysis mode, from 100 to 1200 m/z. LC separation was performed on reversed phase (Zorbax Sb-Aq 100 x 2.1 mm x 1.8 µm particle size), with mobile phases: 0.2% acetic acid (A), and ACN (B). Column oven was kept at 40°C. Ten microliters of aqueous sample (2nd fraction) were injected for metabolite separation with a gradient starting from 2% B, increased to 95% B in 22 min, and maintained during 2 min for column rinsing, followed by column equilibration at 2% B for 4 min. Flow rate was set to 0.3 mL/min. The q-Exactive parameters were: sheath gas flow rate 55 au, auxiliary gas flow rate 15 au, spray voltage 3.3 kV, capillary temperature 300°C, S-Lens RF level 55 V. The mass spectrometer was calibrated with sodium acetate solution dedicated to low mass calibration. Data were analyzed with the quantitative node of Thermo Xcalibur (version 2.2) in a pseudo-targeted approach with a home-based metabolites list.

Proposal model

The proposal model was created with BioRender.com with number of agreement BK246PS4V0.

Data analysis

Data are expressed as means \pm SEM. For statistical analysis, firstly, the normal distribution of the results was evaluated by D'Agostino & Pearson normality test, Shapiro-Wilk normality, and Kolmogorov-Smirnov test. For Gaussian distributions, unpaired two-tailed Student's t-test or one-way analysis of variance (ANOVA) followed by Sidak post hoc multiple comparison test was used for two or multiple comparisons, respectively. For non-Gaussian distributions, the following tests were performed: Mann-Whitney U test was used for two groups and Kruskal-Wallis followed by Dunn post hoc test for multiple groups. Analysis was performed by using the statistical software GraphPad Prism 7. Whole transcriptome sequencing and GEO datasets statistical analysis was tested by Fisher's exact test. For statistical analysis of metabolomic, the p value was calculated by Mann-Whitney test. All targeted treated data were merged and cleaned with a dedicated R (version 3.4) package (@Github/Kroemerlab/GRMeta). A $p < 0.05$ was considered as statistically significant.

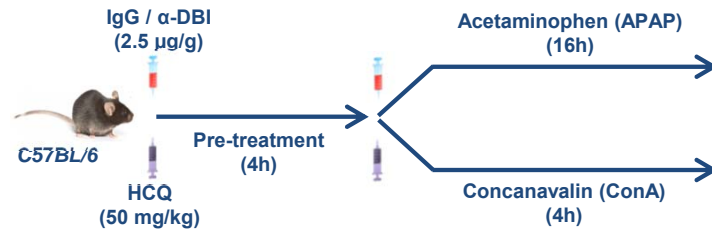
References

1. J. M. Bravo-San Pedro, *et al.*, Acyl-CoA-Binding Protein Is a Lipogenic Factor that Triggers Food Intake and Obesity. *Cell Metab* **30**, 754-767.e9 (2019).
2. P. Wulff, *et al.*, From synapse to behavior: rapid modulation of defined neuronal types with engineered GABAA receptors. *Nat Neurosci* **10**, 923–929 (2007).
3. N. Mizushima, A. Yamamoto, M. Matsui, T. Yoshimori, Y. Ohsumi, In vivo analysis of autophagy in response to nutrient starvation using transgenic mice expressing a fluorescent autophagosome marker. *Mol Biol Cell* **15**, 1101–1111 (2004).
4. M. Tong, *et al.*, Mitophagy Is Essential for Maintaining Cardiac Function During High Fat Diet-Induced Diabetic Cardiomyopathy. *Circ Res* **124**, 1360–1371 (2019).
5. L. Montégut, *et al.*, Immunization of mice with the self-peptide ACBP coupled to keyhole limpet hemocyanin. *STAR Protoc* **3**, 101095 (2022).
6. S. Sciarretta, *et al.*, Trehalose-Induced Activation of Autophagy Improves Cardiac Remodeling After Myocardial Infarction. *J Am Coll Cardiol* **71**, 1999–2010 (2018).
7. S. Venkatesh, *et al.*, Mitochondrial LonP1 protects cardiomyocytes from ischemia/reperfusion injury in vivo. *J Mol Cell Cardiol* **128**, 38–50 (2019).
8. O. Motiño, *et al.*, Protective Role of Hepatocyte Cyclooxygenase-2 Expression Against Liver Ischemia–Reperfusion Injury in Mice. *Hepatology* **70** (2019).
9. O. Motiño, *et al.*, Cyclooxygenase-2 expression in hepatocytes attenuates non-alcoholic steatohepatitis and liver fibrosis in mice. *Biochimica et Biophysica Acta - Molecular Basis of Disease* **1862** (2016).
10. C. G. Tag, *et al.*, Bile Duct Ligation in Mice: Induction of Inflammatory Liver Injury and Fibrosis by Obstructive Cholestasis. *JoVE (Journal of Visualized Experiments)* **96**, e52438 (2015).
11. S. N. Kim, *et al.*, Dose-response Effects of Bleomycin on Inflammation and Pulmonary Fibrosis in Mice. *Toxicological Research* **26**, 217 (2010).
12. W. Liang, *et al.*, Establishment of a general NAFLD scoring system for rodent models and comparison to human liver pathology. *PLoS One* **9** (2014).
13. P. Bedossa, T. Poynard, An algorithm for the grading of activity in chronic hepatitis C. *Hepatology* **24**, 289–293 (1996).
14. S. Suzuki, L. H. Toledo-Pereyra, F. J. Rodriguez, D. Cejalvo, Neutrophil infiltration as an important factor in liver ischemia and reperfusion injury. Modulating effects of FK506 and cyclosporine. *Transplantation* **55**, 1265–1271 (1993).
15. A. Naiki-Ito, *et al.*, Gap junction dysfunction reduces acetaminophen hepatotoxicity with impact on apoptotic signaling and connexin 43 protein induction in rat. *Toxicol Pathol* **38**, 280–286 (2010).

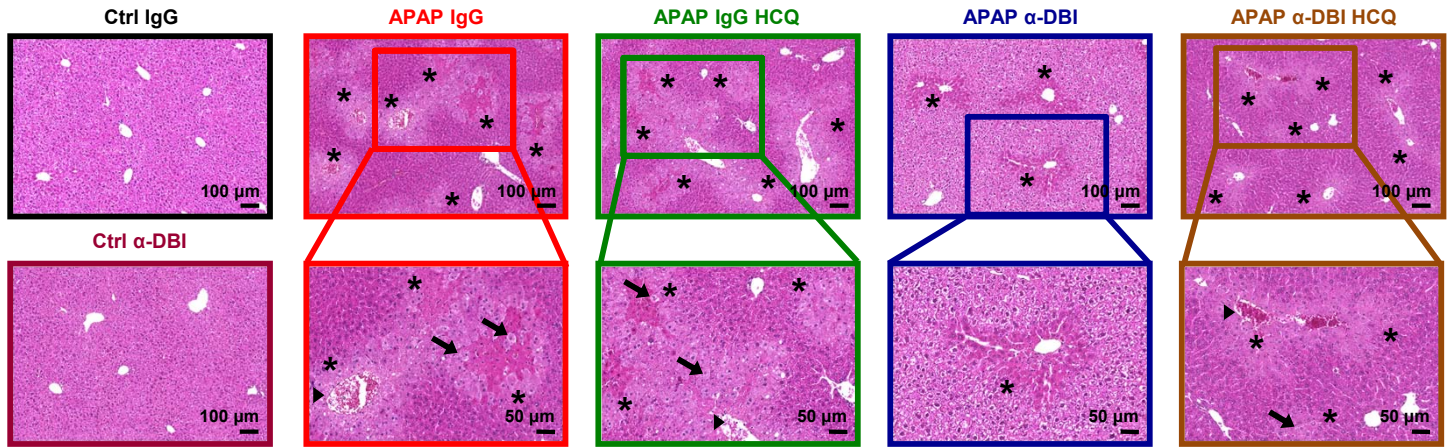
16. J. Zhao, *et al.*, Nicotine attenuates concanavalin A-induced liver injury in mice by regulating the α 7-nicotinic acetylcholine receptor in Kupffer cells. *Int Immunopharmacol* **78** (2020).
17. T. Ashcroft, J. M. Simpson, V. Timbrell, Simple method of estimating severity of pulmonary fibrosis on a numerical scale. *Journal of Clinical Pathology* **41**, 467 (1988).
18. D. Kim, J. M. Paggi, C. Park, C. Bennett, S. L. Salzberg, Graph-based genome alignment and genotyping with HISAT2 and HISAT-genotype. *Nat Biotechnol* **37**, 907–915 (2019).
19. M. I. Love, W. Huber, S. Anders, Moderated estimation of fold change and dispersion for RNA-seq data with DESeq2. *Genome Biol* **15** (2014).
20. J. Wang, S. Vasaikar, Z. Shi, M. Greer, B. Zhang, WebGestalt 2017: a more comprehensive, powerful, flexible and interactive gene set enrichment analysis toolkit. *Nucleic Acids Res* **45**, W130–W137 (2017).
21. C. Grajeda-Iglesias, *et al.*, Oral administration of *Akkermansia muciniphila* elevates systemic antiaging and anticancer metabolites. *Aging* **13**, 6375–6405 (2021).

Figure S1

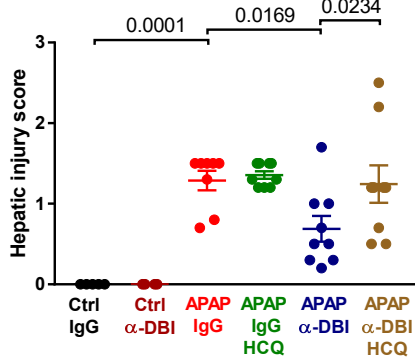
A



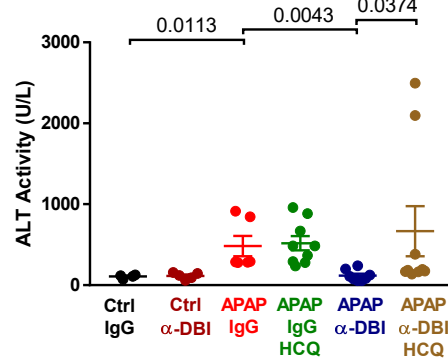
B



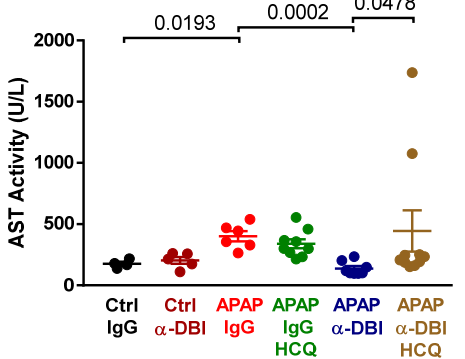
C



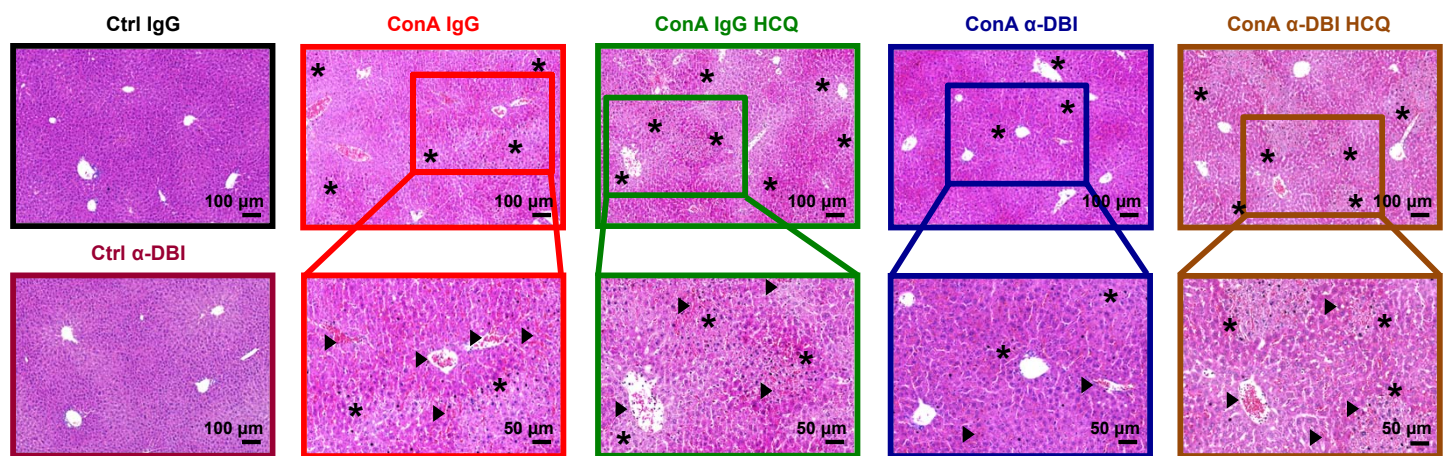
D



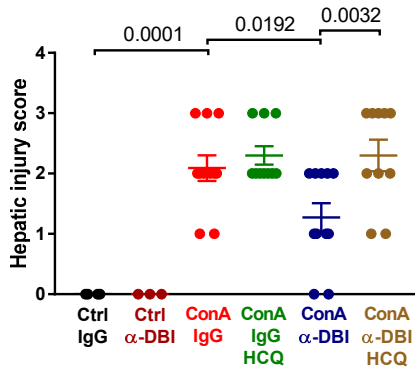
E



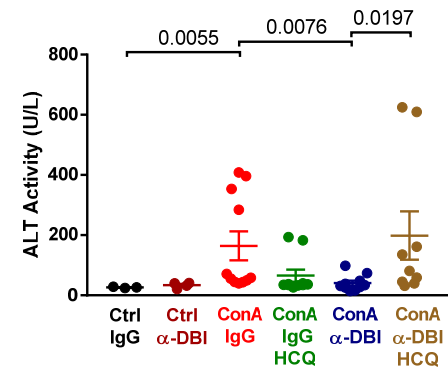
F



G



H



I

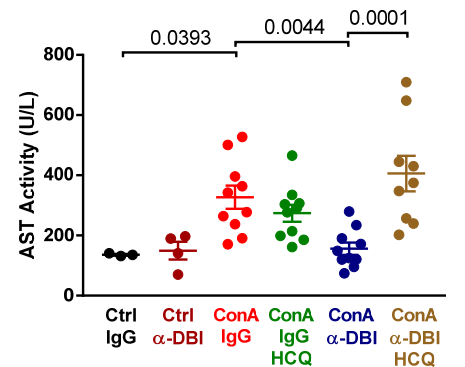


Figure S2

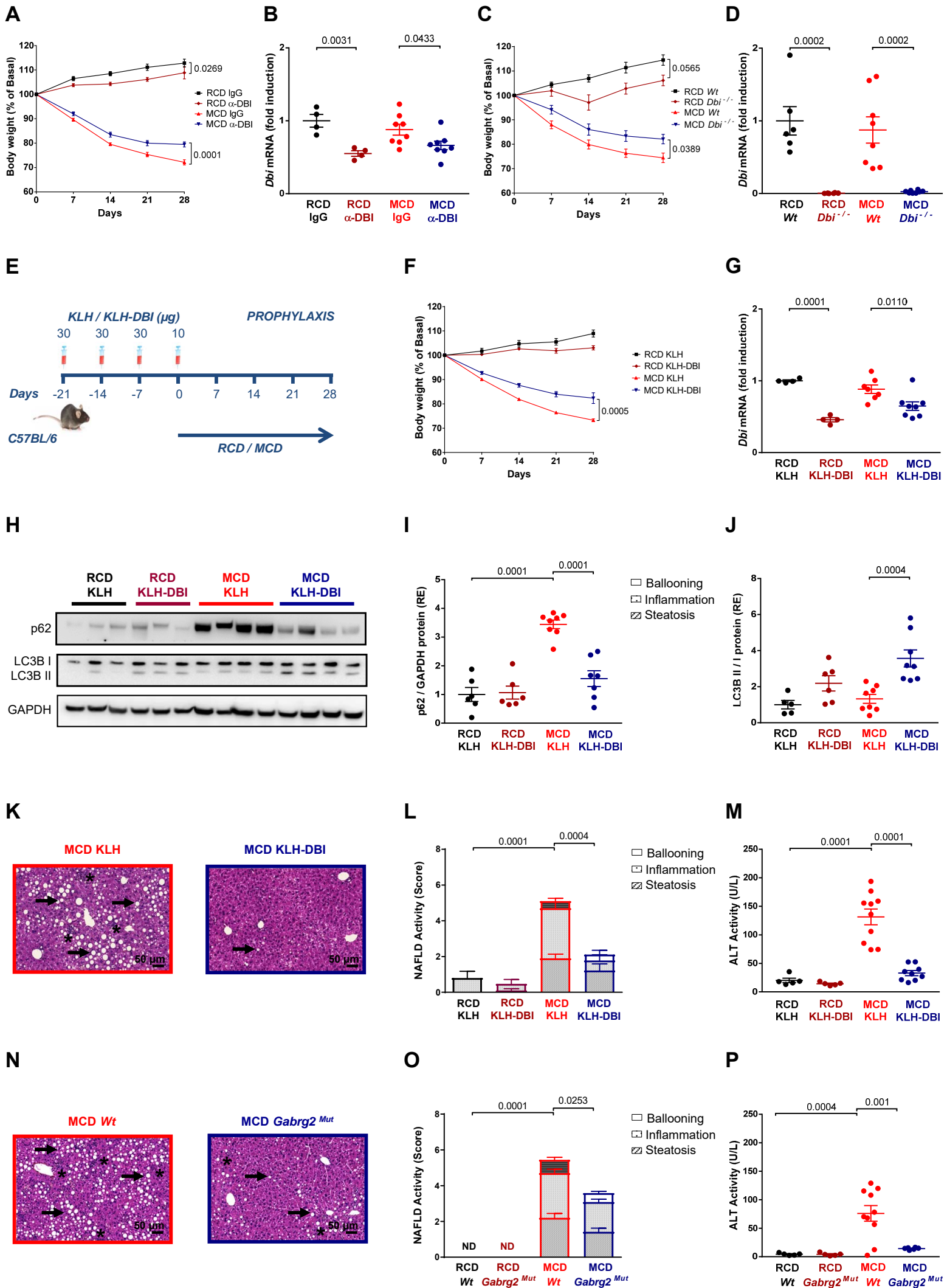
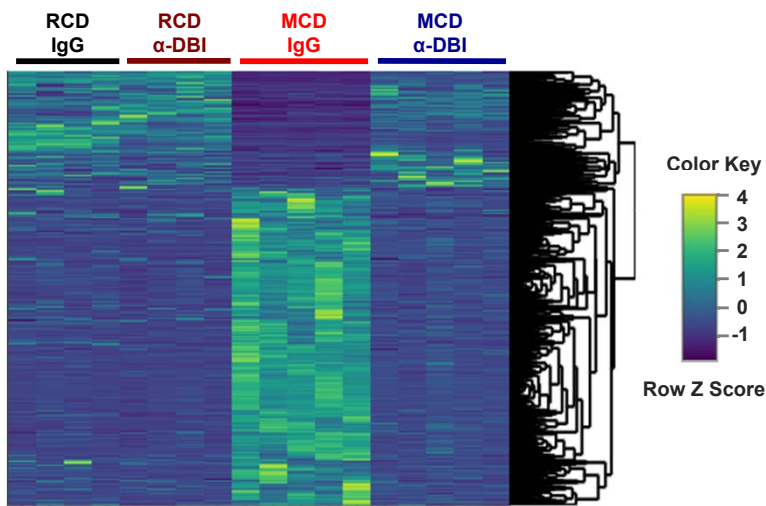
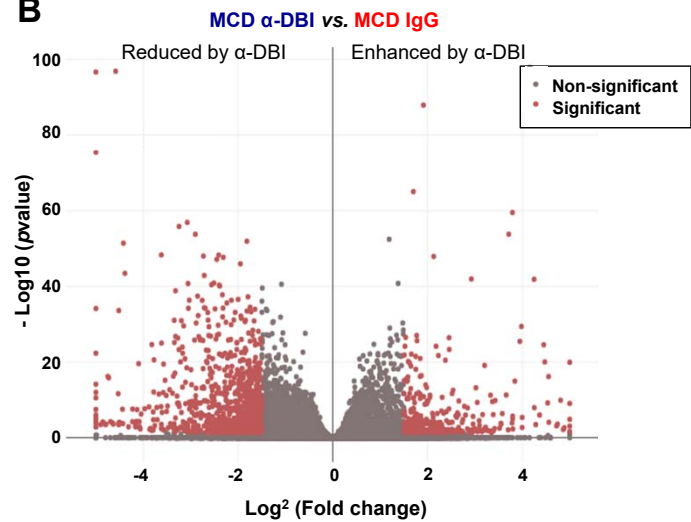


Figure S3

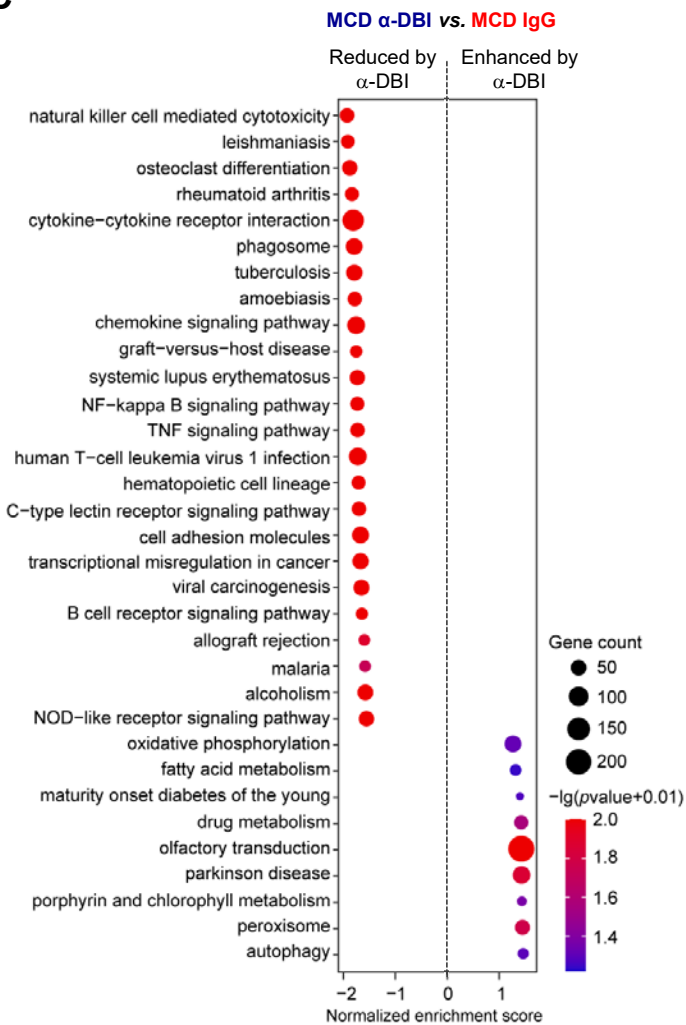
A



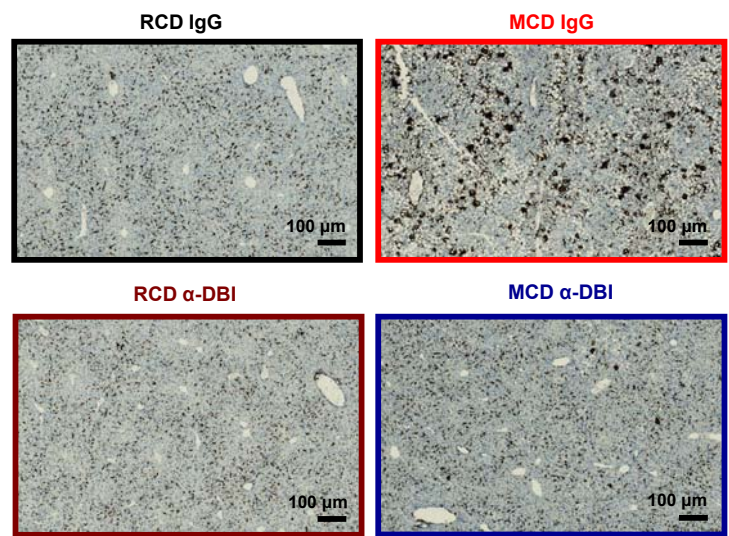
B



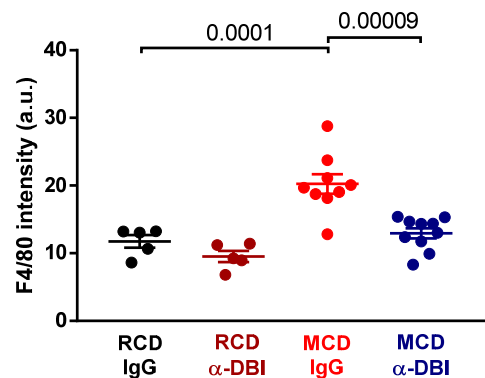
C



D



E



F

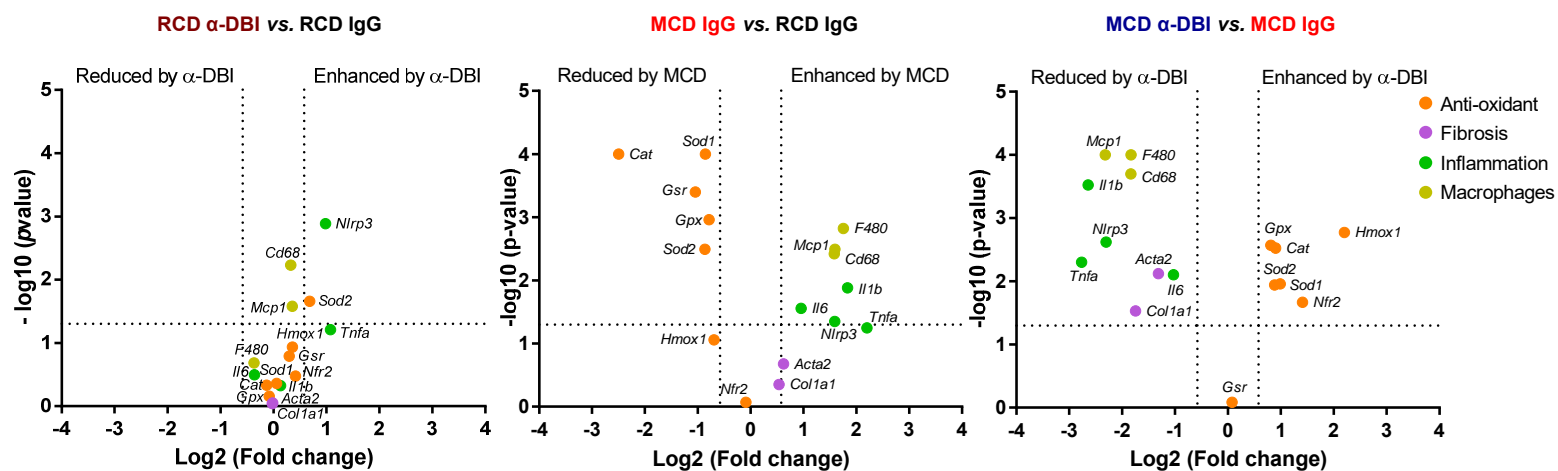
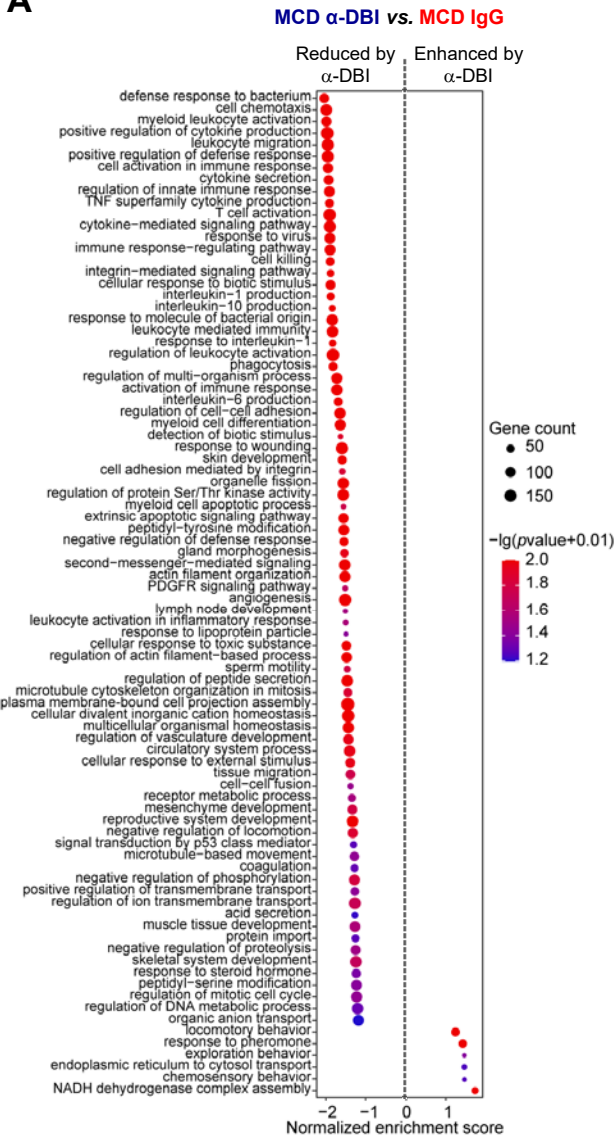
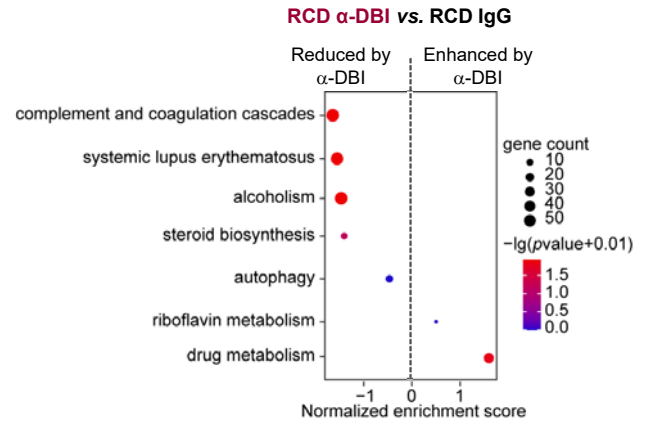


Figure S4

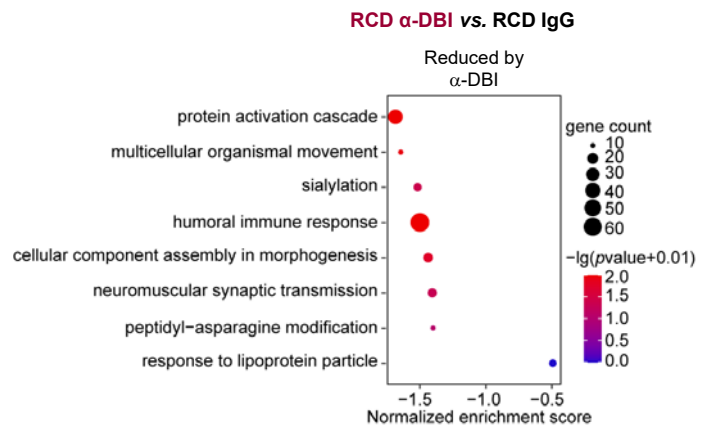
A



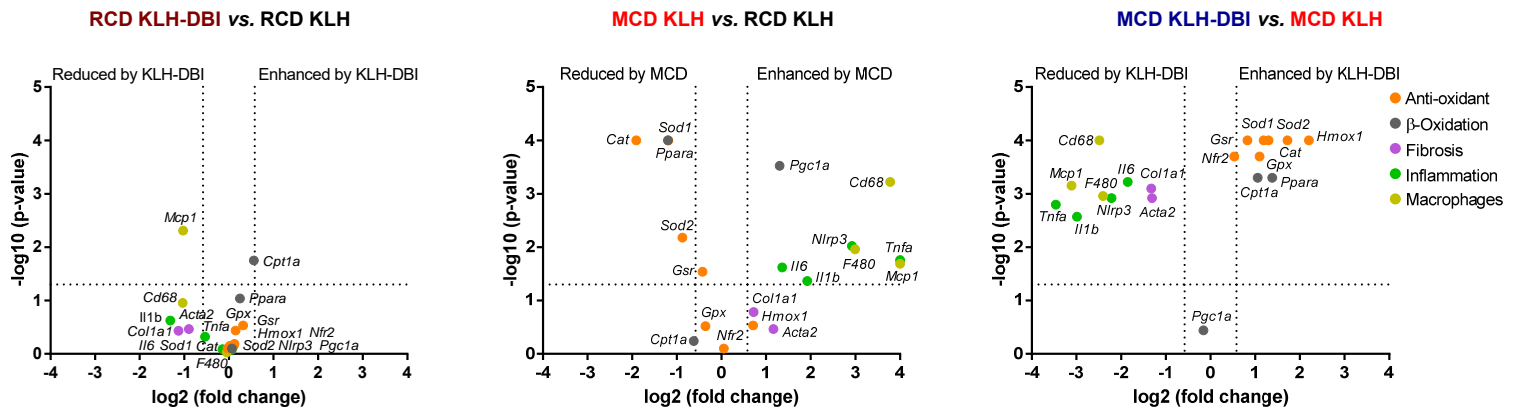
B



C



D



E

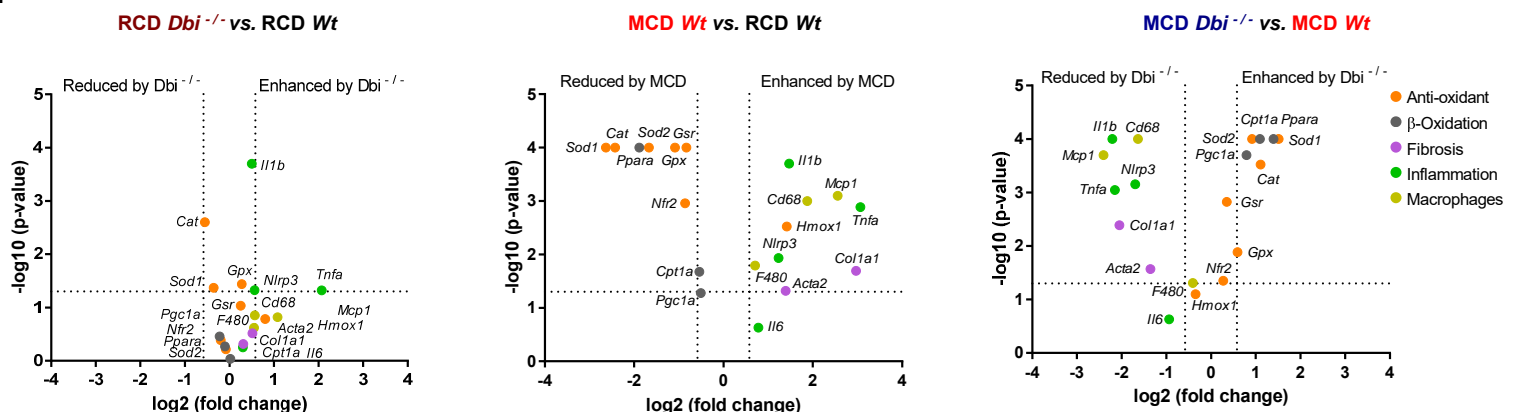
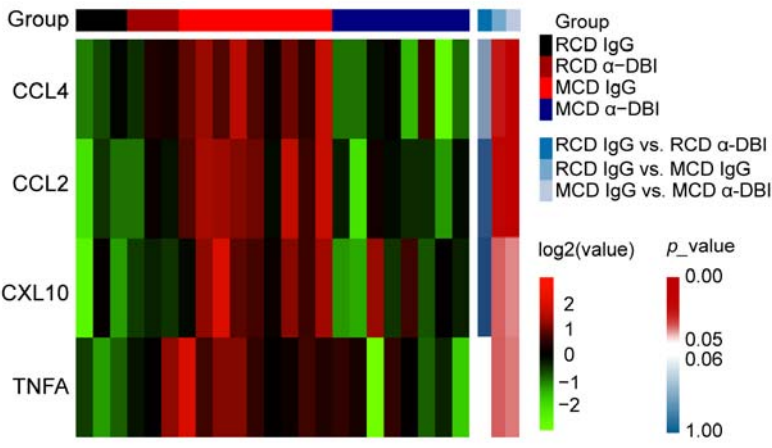
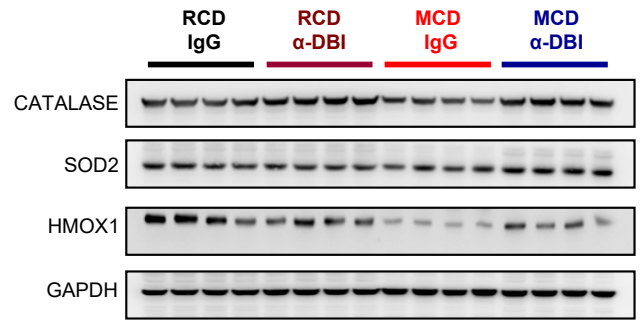


Figure S5

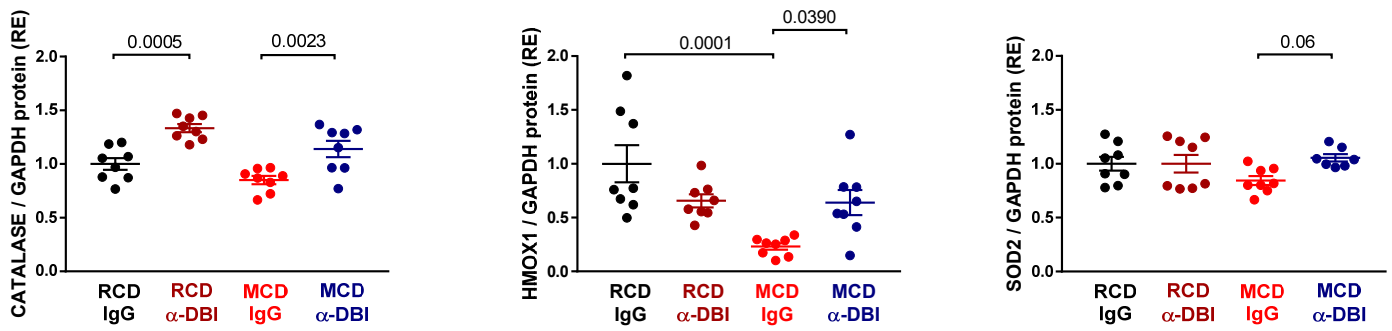
A



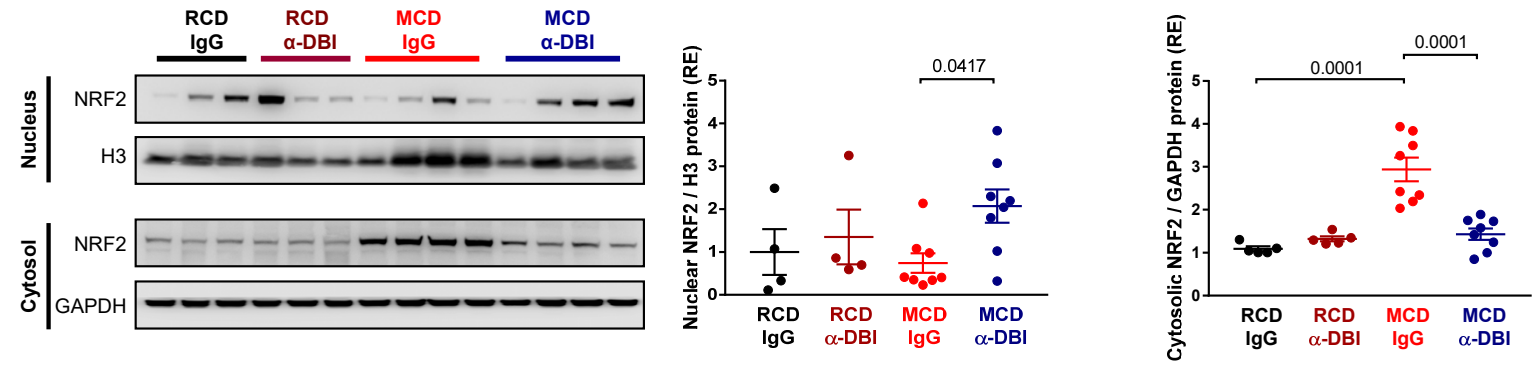
B



C



D



E

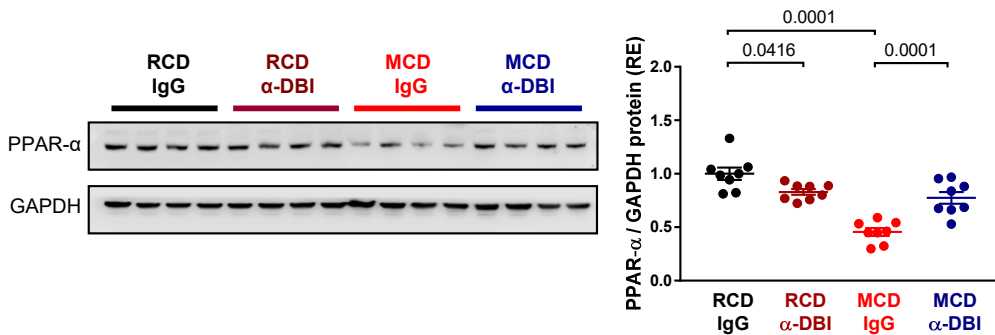
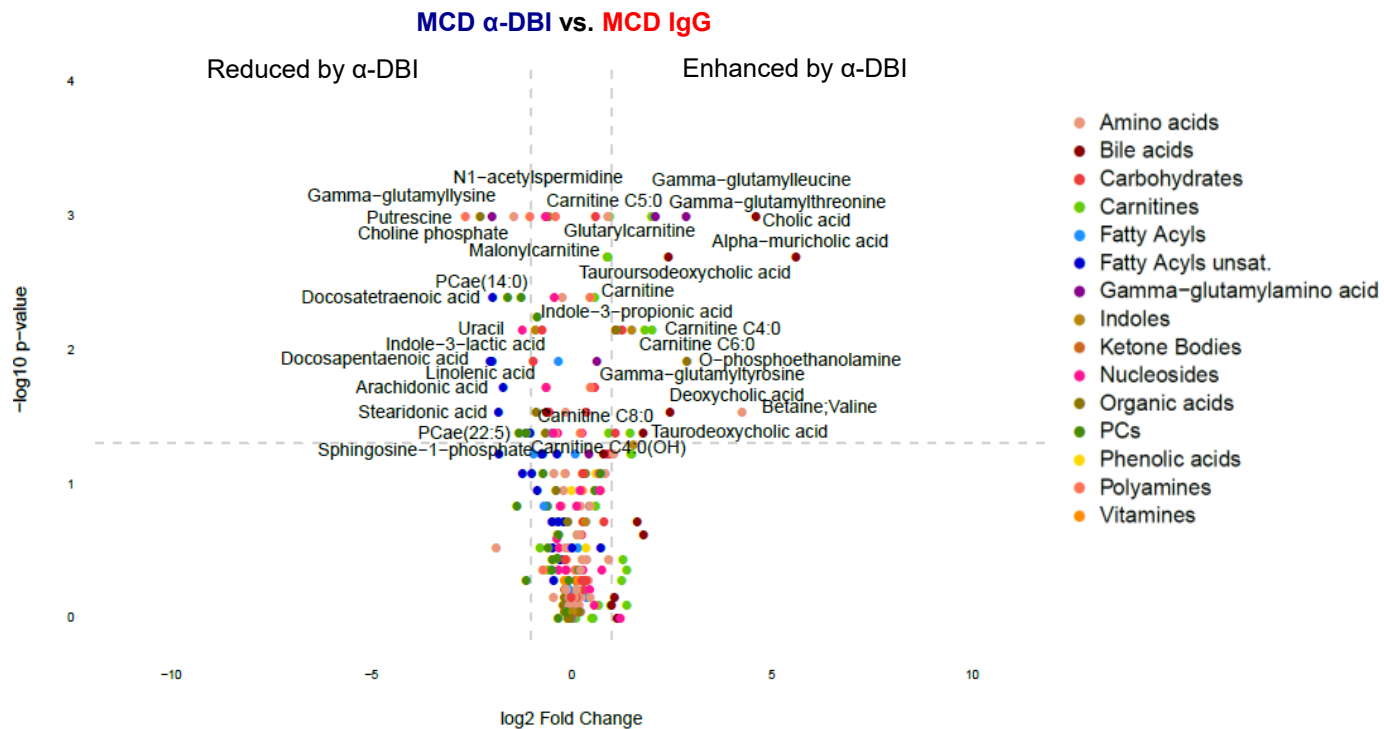
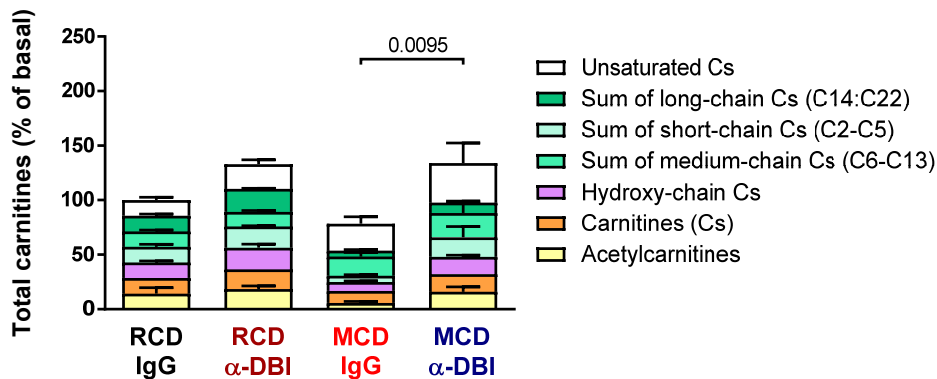


Figure S6

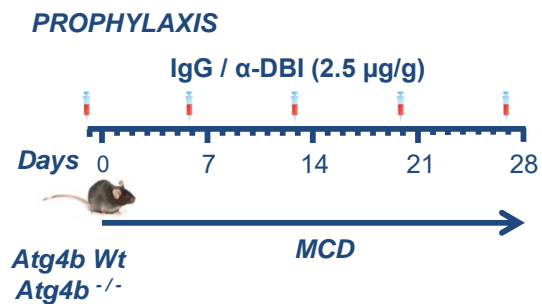
A



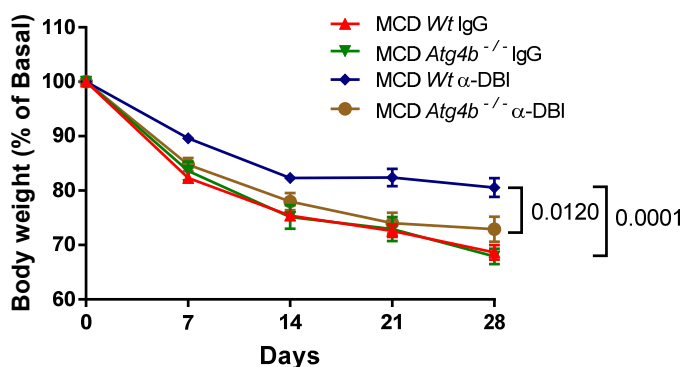
B



C



D



E

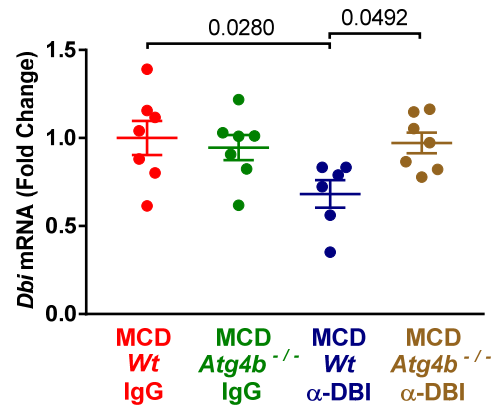
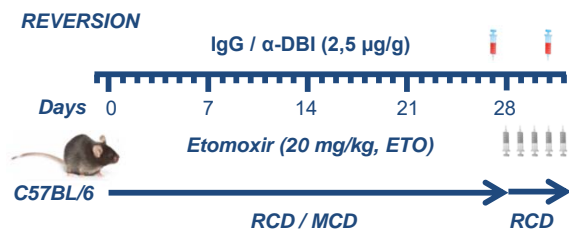
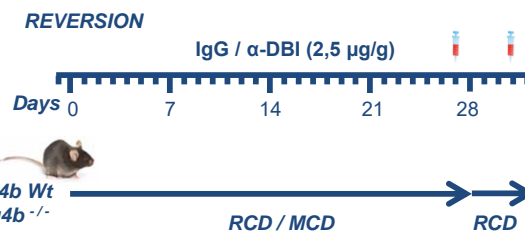


Figure S7

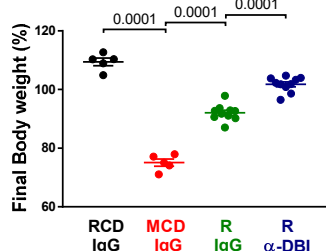
A



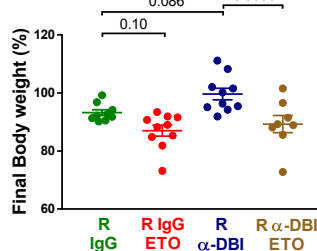
B



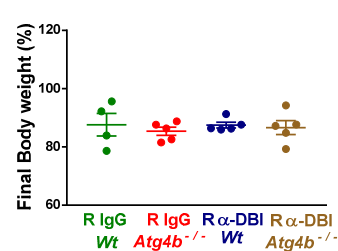
C



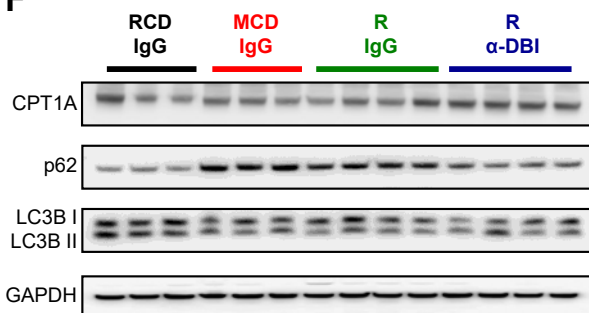
D



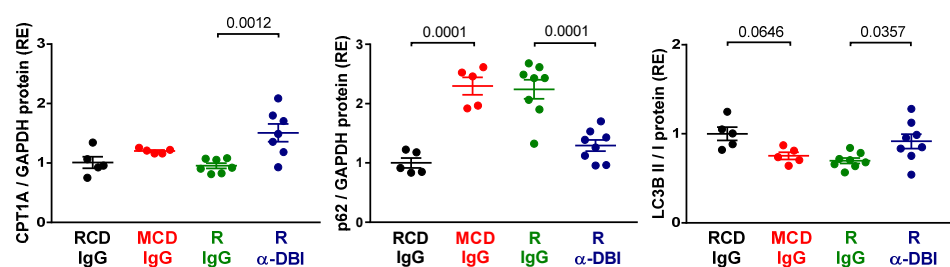
E



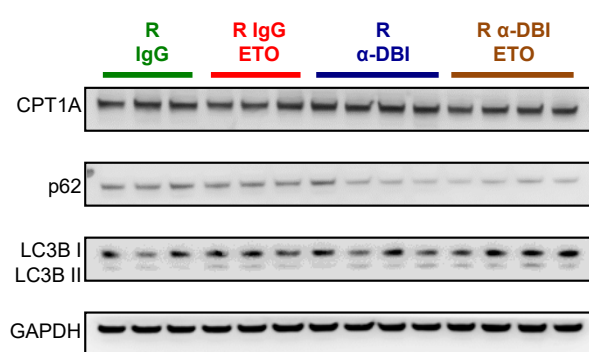
F



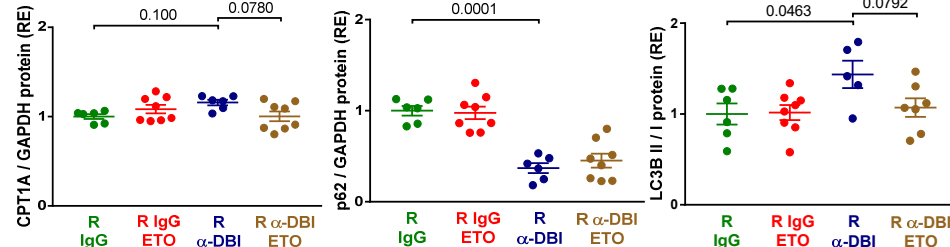
G



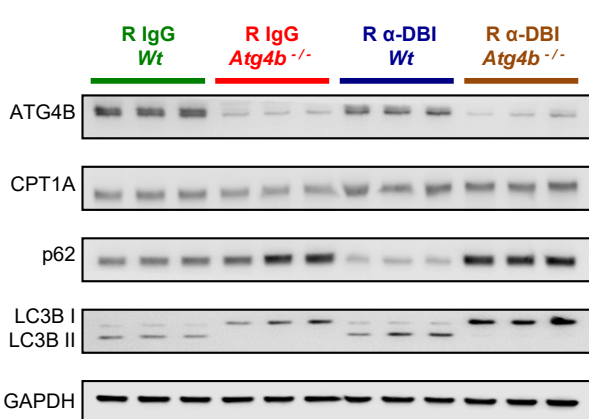
H



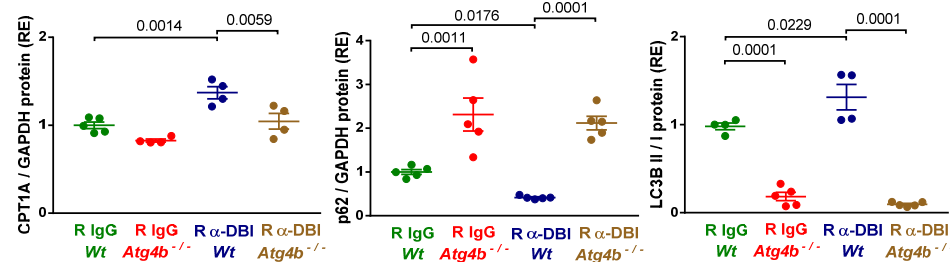
I



K



L



M

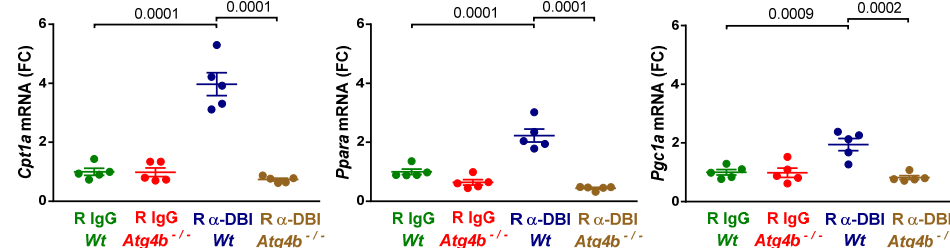
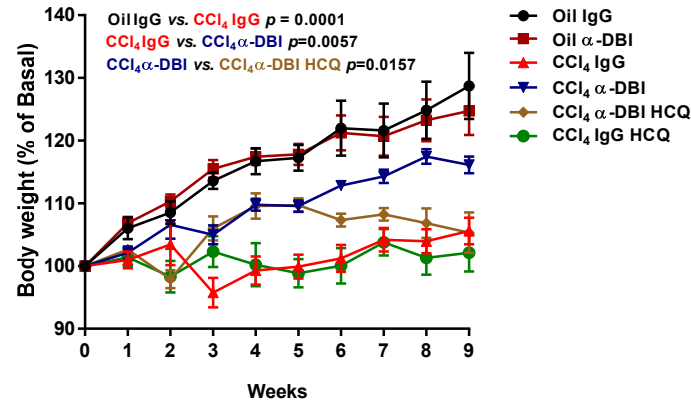
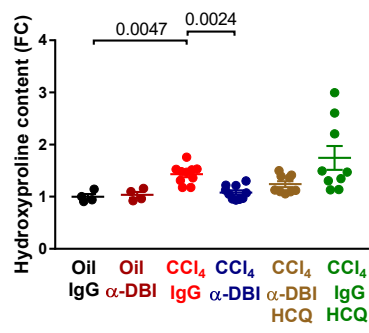


Figure S8

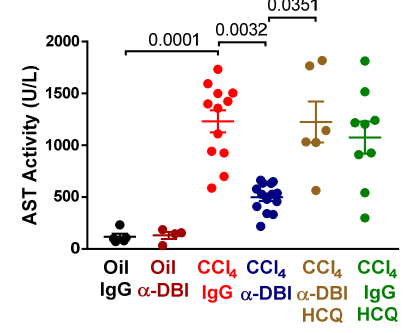
A



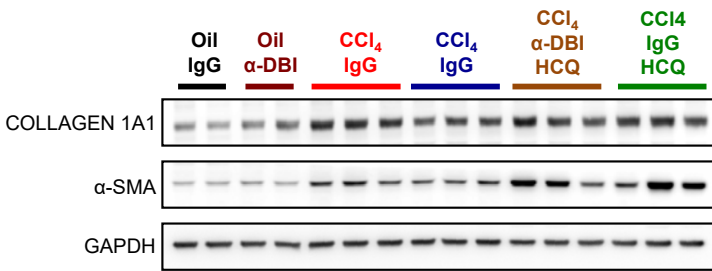
B



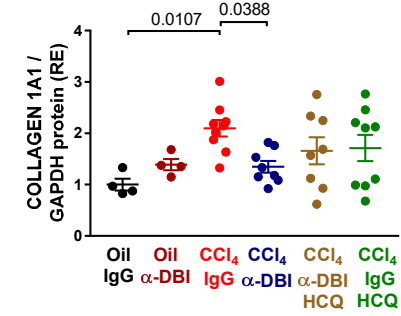
C



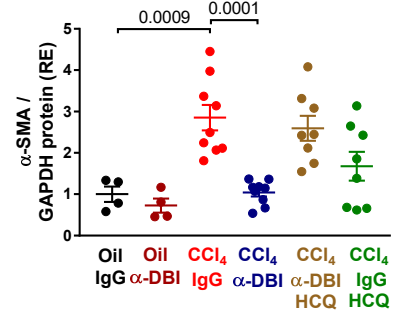
D



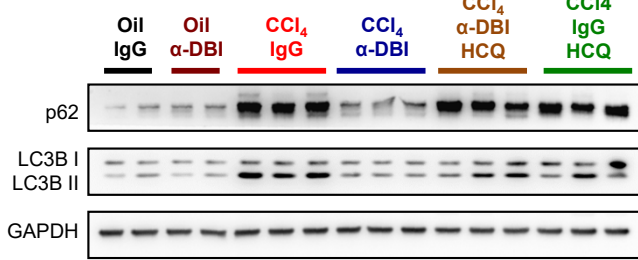
E



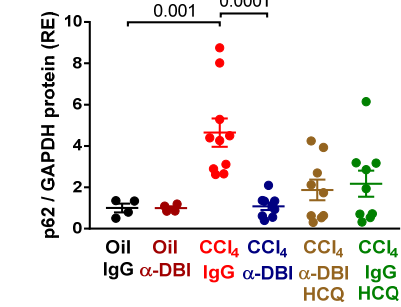
F



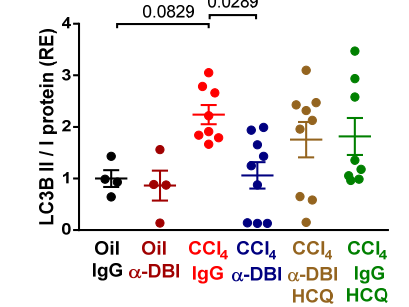
G



H



I



Supplemental Figure Legends

Figure S1. α -DBI alleviates the hepatotoxicity induced by acetaminophen and concanavalin A *in vivo*.

A Experimental procedure of the damage induced by acetaminophen (APAP, i.p. 300 mg/kg for 16 hours) or concanavalin A (ConA, i.v. 12 mg/kg for 4 hours) in mice pre-treated with i.p. injection of α -DBI or IgG (2.5 μ g/g) and HCQ (50 mg/kg) for 4 hours and just before hepatic injury.

B-E Hepatoprotective effect of DBI neutralization after APAP intoxication. Representative images of HES staining (**B**) from mice pre-treated with α -DBI or IgG and HCQ and after APAP. The hepatic injury (**C**) was measured by histological examination taking account the area of cell death, degeneration (ballooning), and inflammation around the central veins. ALT and AST transaminases activity (**D** and **E**) from plasma mice (n=4-9 mice per group).

F-I Liver protection against ConA-damage by DBI neutralization. Histological pictures of HES staining (**F**) from mice pre-treated with α -DBI or IgG and HCQ and after ConA. Liver injury (**G**) was scored using grades of infiltration and hepatocyte necrosis. Activity of ALT and AST transaminases (**H** and **I**) in plasma (n=3-11 mice per group).

Necrotic areas are marked with asterisks, ballooning with arrowheads, and vascular congestion with arrows.

Data are expressed as means \pm SEM. Statistical analyses (*p* values) were performed ANOVA (**C**, **G**, **I**) or Kruskal-Wallis test (**D-E**, **H**).

Figure S2. ACBP/DBI inhibition reduces the loss weight caused by MCD and knockout of ACBP/DBI protects against NASH.

A-D Body weight (**A**) and hepatic mRNA levels of DBI (**B**) from mice treated with α -DBI or IgG as indicated in Fig. 2A (n=4-10 mice per group). Representation of the body weight (**C**) and mRNA levels of *Dbi* in the liver (**D**) from *Dbi*^{-/-} and *Wt* mice (n=6-16 mice per group).

E-N DBI neutralization with antibodies improve NASH damaged derived by MCD. To induce the production of autoantibodies against DBI, the conjugation of recDBI and keyhole limpet hemocyanin (KLH-DBI) or KHL (control) was i.p. administrated weekly to C57BL/6 mice for 4 weeks. After autoimmunization, mice were fed with MCD for 4 weeks (**E**). The body weight (**F**), levels of hepatic *Dbi* mRNA (**G**), representative western blots (**H**) and protein levels of p62 (**I**) and LC3 III/I (**J**) was measured in mice after KLH or KLH-DBI. Histological liver sections stained with HES (**K**), NAFLD activity score (**L**) and plasma ALT (**M**) were analyzed (n=4-10 mice per group). *Wt* and *Gabrg2*^{F771/F771} (*Gabrg2*^{Mut/Mut}) mice were fed with MCD for 4 weeks. HES histology images (**N**), NAFLD score (**O**) and ALT activity (**P**) are shown after MCD (n=5-10 mice per group).

Asterisks, arrows, and arrowheads show inflammation foci, macro-steatosis, and micro-steatosis vesicular, respectively.

Results are displayed as means \pm SEM. Statistical analyses (p value) were calculated by ANOVA test.

Figure S3. Whole transcriptome sequencing reflects a differential gene expression profile in mice treated with α -DBI after MCD.

A-B Heat map (**A**) of the two-way hierarchical clustering (1159 genes satisfying with fold change $\geq \pm 1.5$ and with $p < 0.05$) using Z scores for normalized values from mice fed with RCD or MCD and injected with IgG or α -DBI. Volcano plots comparing mRNA expression levels (**B**) between two groups in mice administrated with α -DBI *versus* IgG and fed with MCD ($n=5$ mice in each group).

C GSEA-based KEGG pathway enrichment analysis for RNA-seq data. RNA-seq was performed to analyze the differential expression of 54325 genes in liver samples obtained from Ig and α -DBI groups with MCD. The most significant pathways are shown.

D-E Representative hepatic images (**D**) and intensity quantification of F4/80 immunohistochemistry (**E**) from all mice on RCD or MCD treated with α -DBI ($n=5-10$ mice per group).

F Analysis of genes involved in inflammation (*Cd68, F480, Il1b, Il6, Mcp1, Nr1p3, Tnfa*), antioxidant responses (*Cat, Hmox1, Nrf2, Gpx, Gsr, Sod1, Sod2*) and fibrosis (*Col1a1, Acta2*) by RT-qPCR. Volcano plots are depicted with the fold change of each gene and the p value was calculated by performing a two-tailed unpaired Student's t test. The setting of threshold for \log^2 (fold change) is ± 0.58 (cut-off value 1.5) and for $-\log_{10}$ (p value) was 1.3 (p value < 0.05). The means of the mRNA expression data were compared between the indicated groups ($n=3-6$ mice per group). Results are represented as means \pm SEM. Statistical analyses (p value) were calculated by Fisher's exact test (**B-C**), ANOVA test (**E**) or two-tailed unpaired Student's t test (**F**).

Figure S4. Analysis of gene expression profile in mice treated with α -DBI after MCD.

A-C GSEA-based KEGG/GO enrichment analysis for RNA-seq data. The differential expression of 54325 genes in liver samples, obtained from MCD plus IgG / α -DBI or RCD plus IgG/ α -DBI groups, were determined by RNA-seq analysis. Then GSEA-based GO enrichment analysis on biological process (**A**: MCD α -DBI vs. MCD IgG; **C**: RCD α -DBI vs. RCD IgG) or KEGG pathway analysis (**B**: RCD α -DBI vs. RCD IgG) were performed to select the significant categories (p value < 0.05 , Fisher's exact test).

D-E Volcano plots of genes related with inflammation (*Cd68, F480, Il1b, Il6, Mcp1, Nr1p3, Tnfa*), antioxidant response (*Cat, Hmox1, Nrf2, Gpx, Gsr, Sod1, Sod2*), fibrosis (*Col1a1 and Acta2*), and β -oxidation (*Cpt1a, Pgc1a, Ppara*) were measured by RT-qPCR. The means of the mRNA expression data were compared between the indicated groups ($n=4-8$ mice per group). p values were calculated by two-tailed unpaired Student's t test.

Figure S5. Analysis of pro-inflammatory cytokines and antioxidant enzymes in mice treated with α -DBI under MCD diet.

A Heatmap clustered by Euclidean distance of the plasmatic levels of CCL4, CCL2, CXCL10 and TNFA assessed by Luminex analysis (n=3-8 mice per group).

B-C Representative immunoblots (**B**) and densitometric analysis of CATALASE, HMOX1 and SOD2 (**C**) (n=7-8 mice per condition).

D Analysis of hepatic NRF2 translocation by Western blot from nuclear and cytosolic extracts (n=4-8 mice per condition).

E Representative Western Blot of PPAR α from total liver extracts (n=8 mice per condition).

Data are expressed as means \pm SEM. Statistical analyses (*p* values) were performed ANOVA.

Figure S6. Effects of α -DBI on liver metabolites.

A-B α -DBI increases the hepatic levels of carnitines. Volcano plot of metabolites (**A**) grouped by categories, comparing MCD-fed mice group treated with α -DBI (n=9) or IgG (n=5). The setting of thresholds for \log^2 (Fold change) is ± 0.58 (cut-off value 1.5) and for $-\text{Log}_{10}$ (*p* value) was 1.3 (*p* value <0.05). Total carnitines and family carnitines are shown (**B**) (n=3-9 per condition).

C-E Schematic figure from *Atg4b*^{-/-} and *Wt* mice treated every week with α -DBI and IgG plus MCD diet for 4 weeks (**C**). Body weight (**D**) and hepatic mRNA levels of *Dbi* (**E**) from mice treated α -DBI and IgG with MCD diet (n=6-8 per group).

Data are displayed as means \pm SEM. Statistical analyses (*p* values) were calculated by means of the two-tailed unpaired Mann Whitney test (**A**) or ANOVA test (**B, D-E**).

Figure S7. α -DBI enhanced the recovery of NASH in an autophagy-dependent fashion.

A-B Experimental strategy of the NASH reversion (R) induced by MCD for 4 weeks plus 4 days with RCD. C57BL/6 (**A**) and *Atg4b*^{-/-} (**B**) mice were injected i.p. with α -DBI or IgG (2.5 $\mu\text{g/g}$) one day before RCD and one day before sacrifice. Additionally, etomoxir (ETO) was administrated i.p every day for 4 days in mice fed with RCD.

C-E Final body weight represented as % of basal body weight from C57BL/6 (**C**) plus ETO (**D**) and *Atg4b*^{-/-} (**E**) mice (n=4-10 mice per group).

F-G Representative immunoblots (**F**) and densitometric quantification (**G**) of CPT1A, p62 and LC3B from liver extracts in mice treated with α -DBI and IgG (n=5-8 mice per condition).

H-I Hepatic CPT1A, p62 and LC3B proteins levels analyzed by Western Blot from C57BL/6 mice treated with α -DBI and IgG plus ETO (n=5-8 mice per treatment).

J mRNA levels of genes involved in β -oxidation such as *Cpt1a*, *Ppara* and *Pgc1a* in the liver (n=5-9 mice per group).

K-M CPT1A, p62 and LC3B proteins levels (**K** and **L**) and *Cpt1a*, *Ppara* and *Pgc1a* mRNA expression (**M**) analyzed by Western Blot and RT-qPCR respectively from liver of *Atg4b*^{-/-} mice treated with α -DBI and IgG (n=4-5 mice per group).

Data are displayed as means \pm SEM. For statistical results, *p* values were calculated by ANOVA test (**C-D**, **G**, **I-J**, **L-M**) or Kruskal-Wallis test (**J**).

Figure S8. ACBP/DBI neutralization prevents hepatic fibrosis in an autophagy-dependent fashion.

A-C Body weight (**A**), levels of hydroxyproline (**B**), and AST activity (**C**) after CCl₄ treatment in prophylaxis model (n=4-14 mice per condition).

D-F Representative Western blot (**D**) and densitometric analysis of COLLAGEN 1A1 (**E**) and α -SMA (**F**) from livers in prophylaxis condition (n=4-10 mice per group).

G-I Liver immunoblots (**G**) and densitometric analysis of p62 (**H**) and LC3B (**I**) from mice treated with α -DBI or IgG plus HCQ in prophylaxis (n=4-10 mice per group).

For statistical analyses, *p* values were calculated by ANOVA test (**A**, **E-F**, **H**) or Kruskal-Wallis test (**B-C**, **I**).

Table S1. ACBP/DBI neutralization downregulates genes that are upregulated in human NAFLD or NASH.

	GEO accession	No. of normal livers (NL)	No. of NASH livers	No. of NAFLD livers	No. of genes over-expressed in NASH/NAFLD (P<0.05)	No. of genes reduced by anti-DBI in mouse MCD (p<0.05)	Overlap between data-sets	No. of genes analyzed in GEO datasets	No. of genes in mouse experiment	No. of unique genes in both groups	Overlap overrepresentation factor*	P value#
1	GSE159676	6	7	—	1484	3987	230	17046	54325	54710	2.13105	6.28E-28
2	GSE151158	21	—	40	239		106	618		54444	6.05636	7.02E-56
3	GSE63067	7	9	—	1587		345	54675		61524	3.35460	4.74E-91
4	GSE48452	14	18	—	1487		360	33297		59696	3.62485	7.04E-106
5	GSE17470	4	7	—	2618		484	44530		59677	2.76717	8.12E-97
6	GSE66676	34	7	26	899		113	28869		59000	1.86005	1.78E-10
7	GSE24807	5	12	—	3333		667	40346		59286	2.97575	6.89E-153
8	GSE33814	13	12	—	4380		1031	48803		58555	3.45702	2.85E-306
9	GSE126848	14	16	15	2581		598	19697		57744	3.35563	1.53E-162
10	GSE135251	10	—	206	4685		931	59913		76362	3.80602	9.39E-300
Sum					13350		2393	46943		84510	3.79947	0

* Overlap overrepresentation factor is ratio between actual overlap over theoretical overlap.

The p values were calculated with Fisher's exact test.

Table S2. List of reagents or resources used in the article.

REAGENT or RESOURCE	SOURCE	IDENTIFIER
Antibodies		
Anti-ACBP/DBI antibody	Abcam	ab231910
Anti- α SMA antibody	Sigma Aldrich	A2547
Anti-ATG4B antibody	Cell Signaling Technology	13507
Anti-CATALASE	Cell Signaling Technology	14097
Anti-COLLAGEN 1A1 antibody	Sigma Aldrich	234167
Anti-CPT1A antibody	Abcam	ab128568
Anti-F4/80 antibody	BioRad	MCA497G
Anti-GAPDH antibody	Cell Signaling Technology	2118
Anti-MAP1LC3B antibody	Cell Signaling Technology	2775
Anti-p62/SQSTM1 antibody	Abnova	H00008878-M01
Anti-PPAR α	Abcam	ab61182
Anti-SOD2	Cell Signaling Technology	13141
Goat Anti-Mouse IgG (H+L) secondary antibody	Southern Biotech	1031-05
Goat Anti-Rat IgG (H+L) secondary antibody	Southern Biotech	3050-05
Goat Anti-Rabbit IgG (H+L) secondary antibody	Southern Biotech	4050-05
IgG2a antibody (in vivo isotype control)	Bioxcell	BE0085
Monoclonal anti-ACBP/DBI (in vivo neutralization)	Fred Hutch Antibody Technology	N/A
Chemicals, Peptides, and Recombinant Proteins		
Acetaminophen (APAP, Paracetamol)	Sigma Aldrich	A7085
Bleomycin (Bleo)	Sigma Aldrich	B5507
Concanavalin (ConA)	Sigma Aldrich	C5275
Etomoxir sodium	Sigma Aldrich	E1905
Hydroxychloroquine sulfate	Axon Medchem BV	2432
Imject mcKLH Subunits	Thermo Scientific	77649

Montanide ISA 51 VG	SEPPIC	36362/FL2R3
Recombinant mouse ACBP/DBI	Custom-made	N/A
SuperSignal West Pico chemiluminescent substrate	Thermo Scientific	34579
SYBR Green Master Mix	Applied Biosystems	4367659
Tamoxifen Free Base	Sigma Aldrich	T5648

Critical Commercial Assays

Alanine transaminase (ALT) kit	Randox	AL1200
Aspartate transaminase (AST) kit	Randox	AS1202
Bilirubin kit	Sigma Aldrich	MAK126
Hydroxyproline kit	Sigma Aldrich	MAK008
Milliplex Mouse Cytokine/Chemokine	Merck Millipore	MCYTMAG-70K-PX32
RNeasy Plus Mini kit	Qiagen	74134
SuperScript™ VILO™ cDNA Synthesis Kit	Invitrogen	11754050

Deposited data

GEO number RNAseq	GSE194346
-------------------	-----------

Experimental models: Organisms/ Strains

<i>Acbp/Dbi</i> ^{fl/fl} mice in which loxP sites flank <i>Acbp</i> exon 2	Ozgene Gift of Dr. Carlos Lopez-Otin, University of Oviedo, Spain	N/A
<i>Atg4b</i> ^{-/-} <i>C57BL/6</i> mice		N/A
<i>Atg7c</i> ^{fl/fl} mice	Tong <i>et al.</i> , 2019	N/A
B6.Cg-Tg(UBC-cre/ERT2)1Ejb/1J mice	Jackson Laboratory, Bar Harbor, ME, USA	N/A
C57BL/6JOlaHsd mice	Envigo	5704F
<i>Gabrg2tm1Wul/J GABAA g2</i> ^{+/+} mice	Charles River Laboratory, Lentilly, France	N/A
<i>Gabrg2tm1Wul/J GABAA g2F771</i> ^{F771} mice	Charles River Laboratory, Lentilly, France	N/A
<i>Mito-Keima</i> Tg mice	Tong <i>et al.</i> , 2019	N/A
<i>GFP-LC3</i> Tg mice	Mizushima <i>et al.</i> , 2004	N/A

Oligonucleotides

qPCR oligonucleotides

<i>Acbp/Dbi</i> : FOR 5' GAATTTGACAAAGCCGCTGAG 3'	This study	N/A
<i>Acbp/Dbi</i> : REV 5' CCCACAGTAGCTTGTGTTGAAGTG 3'	This study	N/A
<i>Acta2</i> : FOR 5' CCCAGACATCAGGGAGTAATGG 3'	This study	N/A
<i>Acta2</i> : REV 5' TCTATCGGATACTTCAGCGTCA 3'	This study	N/A
<i>Cat</i> : FOR 5' GAACGAGGAGGAGAGGAAAC 3'	This study	N/A
<i>Cat</i> : REV 5' TGAAATTCTTGACCGCTTTC 3'	This study	N/A
<i>Cd68</i> : FOR 5' TGTCTGATCTTGCTAGGACCG 3'	This study	N/A
<i>Cd68</i> : REV 5' GAGAGTAACGGCCTTTTTGTGA 3'	This study	N/A
<i>Col1a1</i> : FOR 5' AATGGCACGGCTGTGTGCGA 3'	This study	N/A
<i>Col1a1</i> : REV 5' AGCACTCGCCCTCCCGTCTT 3'	This study	N/A
<i>Col1a2</i> : FOR 5' AGCAGGTCCTTGAAACCTT 3'	This study	N/A
<i>Col1a2</i> : REV 5' AAGGAGTTTCATCTGGCCCT 3'	This study	N/A
<i>Col6a1</i> : FOR 5' TCGGTCACCACGATCAAGTA 3'	This study	N/A
<i>Col6a1</i> : REV 5' TACTTCGGGAAAGGCACCTA 3'	This study	N/A
<i>Col6a2</i> : FOR 5' GCTCCTGATTGGGGGACTCT 3'	This study	N/A
<i>Col6a2</i> : REV 5' CCAACACGAAATACACGTTGAC 3'	This study	N/A
<i>Col6a3</i> : FOR 5' GCTGCGGAATCACTTTGTGC 3'	This study	N/A
<i>Col6a3</i> : REV 5' CACCTTGACACCTTTCTGGGT 3'	This study	N/A
<i>Cpt1a</i> : FOR 5' TCAATCGGACCCTAGACACC 3'	This study	N/A
<i>Cpt1a</i> : REV 5' CTTTCGACCCGAGAAGACCT 3'	This study	N/A
<i>Desmin</i> : FOR 5' GTTTCAGACTTGACTCAGGCAG 3'	This study	N/A
<i>Desmin</i> : REV 5' TCTCGCAGGTGTAGGACTGG 3'	This study	N/A
<i>F4/80</i> : FOR 5' CTTTGGCTATGGGCTTCCAGTC 3'	This study	N/A
<i>F4/80</i> : REV 5' GCAAGGACAGAGTTTATCGTG 3'	This study	N/A
<i>Gpx</i> : FOR 5' ATCGACATCGAACCTGACAT 3'	This study	N/A
<i>Gpx</i> : REV 5' GAGTGCAGCCAGTAATCACC 3'	This study	N/A
<i>Gsr</i> : FOR 5' ATTGGCTGTGATGAGATGCT 3'	This study	N/A
<i>Gsr</i> : REV 5' GGTAGGATGAATGGCAACTG 3'	This study	N/A

<i>Hmox1</i> : FOR 5' AGGCTAAGACCGCCTTCCT 3'	This study	N/A
<i>Hmox1</i> : REV 5' TGTGTTCTCTGTCAGCATCA 3'	This study	N/A
<i>Il1</i> : FOR 5' AGAAGCTGTGGCAGCTACCTG 3'	This study	N/A
<i>Il1</i> : REV 5' GGAAAAGAAGGTGCTCATGTCC 3'	This study	N/A
<i>Il6</i> : FOR 5' GAGGATACCACTCCCAACAGACC 3'	This study	N/A
<i>Il6</i> : REV 5' AAGTGCATCATCGTTGTTTCATACA 3'	This study	N/A
<i>Mcp1</i> : FOR 5' TTA AAAACCTGGATCGGAACCAA 3'	This study	N/A
<i>Mcp1</i> : REV 5' GCATTAGCTTCAGATTTACGGGT 3'	This study	N/A
<i>Nlrp3</i> : FOR 5' ATTACCCGCCCGAGAAAGG 3'	This study	N/A
<i>Nlrp3</i> : REV 5' TCGCAGCAAAGATCCACACAG 3'	This study	N/A
<i>Nrf2</i> : FOR 5' TAGATGACCATGAGTCGCTTGC 3'	This study	N/A
<i>Nrf2</i> : REV 5' GCCAACTTGCTCCATGTCC 3'	This study	N/A
<i>Pdgfa</i> : FOR 5' TGGCTCGAAGTCAGATCCACA 3'	This study	N/A
<i>Pdgfa</i> : REV 5' TTCTCGGGCACATGGTTAATG 3'	This study	N/A
<i>Pdgfb</i> : FOR 5' TTCCAGGAGTGATACCAGCTT 3'	This study	N/A
<i>Pdgfb</i> : REV 5' AGGGGGCGTGATGACTAGG 3'	This study	N/A
<i>Pdgfra</i> : FOR 5' TCCATGCTAGACTCAGAAGTCA 3'	This study	N/A
<i>Pdgfra</i> : REV 5' TCCCGGTGGACACAATTTTTTC 3'	This study	N/A
<i>Pdgfrb</i> : FOR 5' TTCCAGGAGTGATACCAGCTT 3'	This study	N/A
<i>Pdgfrb</i> : REV 5' AGGGGGCGTGATGACTAGG 3'	This study	N/A
<i>Pgc1a</i> : FOR 5' AAGTGTGGA ACTCTCTGGA ACTG 3'	This study	N/A
<i>Pgc1a</i> : REV 5' GGGTTATCTTGGTTGGCTTTATG 3'	This study	N/A
<i>Ppara</i> : FOR 5' AGAGCCCCATCTGTCCTCTC 3'	This study	N/A
<i>Ppara</i> : REV 5' ACTGGTAGTCTGCAAAACCAAA 3'	This study	N/A
<i>Sod1</i> : FOR 5' TGTGTCCATTGAAGATCGTG 3'	This study	N/A
<i>Sod1</i> : REV 5' CTTTGCCCAAGTCATCTTGT 3'	This study	N/A
<i>Sod2</i> : FOR 5' TCAGTGCTCACTCGTGTCAT 3'	This study	N/A
<i>Sod2</i> : REV 5' ACACGATAGGTTTGGGCATA 3'	This study	N/A

<i>Tnfa</i> : FOR 5' CATCTTCTCAAAATTCGAGTGACAA 3'	This study	N/A
<i>Tnfa</i> : REV 5' TGGGAGTAGACAAGGTACAACCC 3'	This study	N/A
<i>Vimentin</i> : FOR 5' CGTCCACACGCACCTACAG 3'	This study	N/A
<i>Vimentin</i> : REV 5' GGGGGATGAGGAATAGAGGCT 3'	This study	N/A
<i>Rplo/36b4</i> : FOR 5' ACTGGTCTAGGACCCGAGAAG 3'	This study	N/A
<i>Rplo/36b4</i> : REV 5' TCCCACCTTGTCTCCAGTCT 3'	This study	N/A

Genotyping

<i>Cre</i> : FOR 5' AGGTTTCGTTCACTCATGGA 3'	This study	N/A
<i>Cre</i> : REV 5' TCGACCAGTTTGTACCC 3'	This study	N/A
<i>GABRG2</i> knock-in: FOR 5' AAGCGCCACCTCTACTTCT 3'	This study	N/A
<i>GABRG2</i> knock-in: REV 5' TCATGGGATAGTGCATCAGC 3'	This study	N/A

Software and algorithms

DESeq2 package	Love et al., 2014	N/A
Gene Ontology analysis (http://www.bioinformatics.com.cn)	Wang et al., 2017	N/A
HISAT2 algorithm (reference genome GRCm39)	Kim et al., 2019	N/A
Image J	National Institutes of Health	N/A
Metabolomic dataset analysis R (v3.4) package (@Github/Kroemerlab/GRMeta)		
GraphPad Prism 7 software	Graph Pad Software Inc Centre for Cancer Research & Cell Biology at Queen's University Belfast	N/A
QuPath 0.2.3 software		N/A
StepOne Software v2.3	Applied Biosystems	N/A
Zen 3.2 software	ZEISS	N/A

Others

Precellys tissue homogenizing ceramic beads	Bertin Technologies	CKMix
Lithium heparin blood collection tubes	Sarstedt	6443
Luminex™ FLEXMAP 3D™ Instrument System	Merck Millipore	APX1342
Methione and choline deficiente diet (MCD)	Safe	AIN-76

Regular-chow Diet (RCD)
StepOnePlus Real-Time PCR System

Safe
Applied Biosystems

A04
N/A